Appendix 1

During the three years of the PhD course, in addition to the main project, I also followed other research projects.

Microbial Bioelectricity

The first concerned the production of electricity by bacteria starting from organic matter in devices known as microbial fuel cells (MFC)(Lovley, 2006).

Figure 15 shows a schematic diagram of a typical MFC for producing electricity. It consists of anodic and cathodic chambers partitioned by a proton exchange membrane. Microbes in the anodic chamber oxidize added substrates and generate electrons and protons in the process. The electrons are transferred (through different mechanisms) to the anodic electrode and flow through an external circuit to the cathode where they combine with protons and a chemical catholyte such as oxygen, producing electricity (Du *et al.*, 2007).

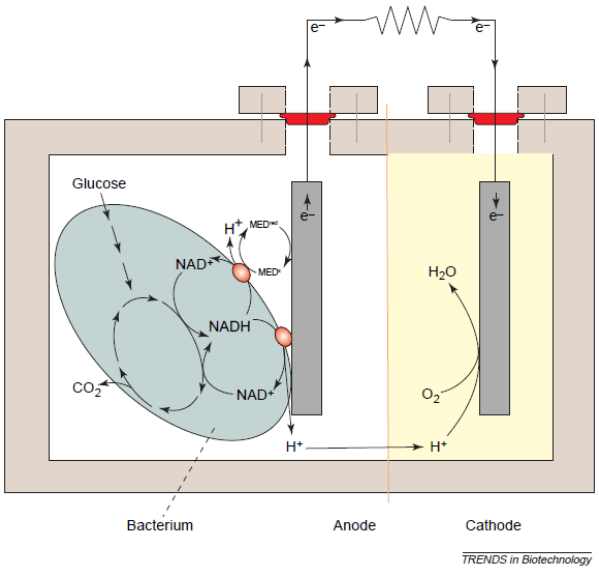

Figure 15 : The working principle of a microbial fuel cell. Substrate is metabolized by bacteria, which transfer the gained electrons to the anode. This can occur either directly through the membrane or via mobile redox shuttles. MED, redox mediator; Red oval, terminal electron shuttle in or on the bacterium [From (Rabaey & Verstraete, 2005)].

Two principal mechanisms used by microorganisms to transfer electrons to electrodes have emerged to date. The first is indirect and involves the use of mediators, called "*shuttle*". These electron shuttles are typically capable of crossing cell membranes, accepting electrons from one or more electron carriers within the cell, exiting the cell in the reduced form and then transferring electrons onto the electrode surface. Then they can re-enter the cell in the oxidized form, charging electron again and transport them outside. These mediators may be exogenous or in some instances, microorganisms might produce their own mediators (Lovley, 2006). The second mechanism (used by real electricigens) is direct. In this case bacteria form biofilms on the electrode surface and the electrons are transferred by the individual cells to the electrode or directly through outer-membrane c-type cytochromes, or through extracellular polymeric substances and specialized micropili that act as real microscopic electrical cables (called "nanowires") and that connect the bacterial cells between them and to the electrode. This second mechanism is much more efficient and less expensive than the previous one (Lovley, 2006, Bond *et al.*, 2012).

Much of the research on MFCs focused on improving the hardware of the cells and various types of MFC have been compared in terms of their performance relating to power generation and energy source (Rabaey & Verstraete, 2005, Kim *et al.*, 2007, Logan, 2010), while few studies investigated the changes in the microbial communities and organic matter characteristics following MFC treatment. In particular, it is still not clear how widespread electrogenic bacteria are in the environment. Initially it was thought that current production might be a rare trait in microorganisms, limited only to some “electroactive” anaerobic species such as *Geobacter* or *Shewanella* (Bond & Lovley, 2003, Logan *et al.*, 2005). However, subsequent studies showed that the electrogenic properties are not exclusive to a few bacterial species but are much more widespread and variable than previously thought, that different bacteria are "specialized" for the use of different organic

substrates and complex organic matrices that are oxidized and used as a nutrient by whole microbial communities constituted by many different bacteria, each of which is specialized for a specific function. Therefore research is now no longer directed towards a single electrogenic bacterium, to be used with any biomass, but towards different bacteria, or more often bacterial communities, specialized for certain types of organic substances. The aim is therefore to identify the most efficient microorganisms in the use of specific substrates. These substrates can be simple (eg. Glucose, acetate etc.) or waste biomass with an highly complex and heterogeneous composition (Logan & Regan, 2006).

Within the BEM (BioElettricità Microbica) project funded by Italian Ministry of Agricultural, Food, and Forestry Policies (MIPAAF), the anodic chamber of MFCs was supplied directly with a natural soil (S) and compared to MFCs supplied with a composted organic fertilizer (A), a complex organic matrix with an high amount of organic matter. The aims were to check whether these aerobic organic matrices could contain electroactive bacteria and to isolate and identify the culturable bacterial species that might be related to any chemical change of OM stimulated by MFCs operated under electricity generating conditions. Our research group was involved in the characterization of the cultivable microbial community.

Although the aim of the study was not to optimize power generation, both the current density and the pattern of electricity production detected were consistent to those observed by other authors.

The alterations of microbial diversity were evaluated for both total and culturable bacterial fractions during the anodic incubation of S and A. Denaturing gradient gel electrophoresis revealed a significant alteration of the microbial community structure in MFCs generating electricity as compared with no-current-producing MFCs, while the genetic diversity of cultivable bacterial communities was assessed by random amplified polymorphic DNA (RAPD) analysis of 106 bacterial isolates obtained by using both generic and elective media. Sequencing of the 16S rRNA

genes of the more representative RAPD groups indicated that over 50.4% of the isolates from MFCs fed with S were Proteobacteria (25.1% Firmicutes, and 24.5% Actinobacteria) whereas in MFCs supplied with A 100% of the dominant species belonged to γ- Proteobacteria.

The chemical analysis performed by fractioning the organic matter and using thermal analysis showed that the amount of total organic carbon contained in the soluble phase of the electrochemically active chambers significantly decreased as compared to the no-current-producing systems, whereas the organic matter of the solid phase became more humified and aromatic along with electricity generation, suggesting a significant stimulation of a humification process of the OM.

Then, data obtained demonstrated that electroactive bacteria are commonly present in aerobic organic substrates such as soil or a fertilizer and that MFCs could represent a powerful tool for exploring the mineralization and humification processes of the soil OM.

Appl Microbiol Biotechnol
DOI 10.1007/s00253-012-3906-6

ENVIRONMENTAL BIOTECHNOLOGY

Alteration of bacterial communities and organic matter in microbial fuel cells (MFCs) supplied with soil and organic fertilizer

Stefano Mocali · Carlo Galeffi · Elena Perrin · Alessandro Florio · Melania Migliore · Francesco Canganella · Giovanna Bianconi · Elena Di Mattia · Maria Teresa Dell'Abate · Renato Fani · Anna Benedetti

Received: 25 October 2011 / Revised: 12 January 2012 / Accepted: 16 January 2012

Abstract The alteration of the organic matter (OM) and the composition of bacterial community in microbial fuel cells (MFCs) supplied with soil (S) and a composted organic fertilizer (A) was examined at the beginning and at the end of 3 weeks of incubation under current-producing as well as no-current-producing conditions. Denaturing gradient gel electrophoresis revealed a significant alteration of the microbial community structure in MFCs generating electricity as compared with no-current-producing MFCs. The genetic diversity of cultivable bacterial communities was assessed by random amplified polymorphic DNA (RAPD) analysis of 106 bacterial isolates obtained by using both generic and elective media. Sequencing of the 16S rRNA genes of the more representative RAPD groups indicated that over 50.4% of the isolates from MFCs fed with S were *Proteobacteria*, 25.1% Firmicutes, and 24.5% *Actinobacteria*, whereas in MFCs supplied with A 100% of the dominant species belonged to γ-*Proteobacteria*. The chemical analysis performed by fractioning the OM and using thermal analysis showed that the amount of total organic carbon contained in the soluble phase of the electrochemically active chambers significantly decreased as compared to the no-current-producing systems, whereas the OM of the solid phase became more humified and aromatic along with electricity generation, suggesting a significant stimulation of a humification process of the OM. These findings demonstrated that electroactive bacteria are commonly present in aerobic organic substrates such as soil or a fertilizer and that MFCs could represent a powerful tool for exploring the mineralization and humification processes of the soil OM.

Keywords Microbial fuel cells · Soil · Organic matter · Electrogenic bacteria · Microbial diversity · Humification

Electronic supplementary material The online version of this article (doi:10.1007/s00253-012-3906-6) contains supplementary material, which is available to authorized users.

S. Mocali (✉)
CRA—Agrobiology and Pedology Research Centre,
Piazza D'Azeglio, 30,
50121 Firenze, Italy
e-mail: stefano.mocali@entecra.it

S. Mocali · C. Galeffi · A. Florio · M. Migliore · M. T. Dell'Abate · A. Benedetti
CRA—Research Centre for the Soil–Plant System,
via della Navicella 2,
00184 Roma, Italy

E. Perrin · R. Fani
Evolutionary Biology Department, University of Florence,
via Romana 17-19,
50125 Firenze, Italy

F. Canganella · G. Bianconi
Department for Innovation in Biological,
Agrofood and Forest systems, University of Tuscia,
via C. de Lellis,
01100 Viterbo, Italy

E. Di Mattia
Department of Sciences and Technologies for Agriculture,
Forest, Nature and Energy, University of Tuscia,
via C. de Lellis,
01100 Viterbo, Italy

Published online: 31 January 2012

Introduction

Microbial fuel cells (MFCs) are devices that use bacteria to directly generate current through catalytic oxidation of

organic matter (OM) under anaerobic conditions (Logan 2009). Electrons removed by "exoelectrogenic" bacteria from these substrates are transferred to the anodic electrode and flow through an external circuit to the cathode where they combine with protons and a chemical catholyte such as oxygen, producing electricity. These systems have recently been of great interest as a potential candidate for future alternative energy and production (Lovley 2008; Logan 2010). In fact over the past years several studies have demonstrated that MFCs can be used to harvest biologically generated electricity from a number of organic and inorganic compounds (Pant et al. 2010) or complex organic wastes such as wastewaters (Liu et al. 2004; Min et al. 2005), marine or freshwater sediments (Reimers et al. 2001; Tender et al. 2002; Bond et al. 2002; Holmes et al. 2004; Mathis et al. 2008), agricultural biomasses (Niessen et al. 2004; Zuo et al. 2006; Scott and Murano 2007; Zhang et al. 2009), and even rhizodeposits (De Schamphelaire et al. 2008) or marine plankton (Reimers et al. 2007). The flexibility of microorganisms to use a range of such organic molecules as fuel makes the MFC device an intriguing technology for renewable bioelectricity generation from waste biomasses. However, to date the current and power densities achieved with MFCs are relatively low as multiple factors limit the performance of the system (Logan and Regan 2006a; Kim et al. 2007a).

Although much of the research on MFCs is focused on improving the hardware of the cells and various types of MFC have been compared in terms of their performance relating to power generation and energy source (Rabeay and Vestraete 2005; Scott and Murano 2007; Kim et al. 2007a; Logan 2010), few studies investigated the changes in both microbial communities and OM characteristics following MFC treatment. For example, some studies have been conducted in order to exploit the correlation between the exoelectrogenic bacterial diversity and the OM quality in marine environments (Brüchert and Arnosti 2003; Reimers et al. 2007) but to date poor work have been done with soil. Moreover, it is still not clear how widespread exoelectrogenic bacteria are in the environment. In early fuel cell studies some results suggested that current production might be a rare trait in microorganisms, limited only to some "electroactive" anaerobic species such as *Geobacter* (Bond and Lovley 2003) or *Shewanella* (Logan et al. 2005). However mixed cultures, or microbial consortia, have been shown to be more efficient and productive than single strains (Phung et al. 2004; Aelterman et al. 2006; Logan and Regan 2006b; Rabaey et al. 2007) and the analysis of the anodic communities revealed a diversity of bacteria much greater than expected, which varied with different inocula and energy sources on the anode surface (Kim et al. 2006, 2007b; Rabaey et al. 2007; Rismani-Yazdi et al. 2007; Ishii et al. 2008). The microbial communities contributing to current production are functionally complex and just some microorganisms can be a significant contributor to direct power production which can change with various fuel sources. To date the ecological role of these communities remains unknown because of the lack of direct functional correlation with phylogenetic identity, the oxidation process of the fuel source, and the possibility of other metabolisms that do not generate electricity.

As the microbial diversity in MFCs is strictly dependent on the amount and on the quality of OM (Phung et al. 2004; Hong et al. 2010), in this study the anodic chamber of MFCs was supplied directly with a natural soil (S), one of the most important natural sources of bacterial diversity (Sleator et al. 2008), and compared to MFCs supplied with a composted organic fertilizer (A), a complex organic matrix with an high amount of OM, in order to accomplish a selection of environmental microbial communities involved in the electrogenic process while, at the same time, relating their genetic and functional diversity to the OM's mineralization process. The specific objectives of this study were to check whether aerobic organic matrices such as soil or a fertilizer could contain electroactive bacteria and to isolate and identify the culturable bacterial species that might be related to any chemical change of OM stimulated by MFCs operated under electricity generating conditions. The alterations of microbial diversity were evaluated by molecular characterization of both total and culturable bacterial fractions during the anodic incubation of S and A. In order to comprehend which part of organic substrates are preferentially degraded after MFC operation the OM was characterized with respect to its chemical–physical properties. In particular the OM in the MFCs at the end of incubation was subjected to a sequential chemical fractionation based on differences in solubility in water, alkaline, and acid conditions, in order to investigate any modifications induced to the most stable and humified organic matter fraction by the electricity generation. Among the several available analytical techniques, thermal analysis (DSC: differential scanning calorimetry; TG: thermogravimetry) have been also chosen as already successfully used to chemically characterize complex organic compounds such as compost, soil organic matter and humic substances (Dell'Abate et al. 2000; Lluch et al. 2005; Klammer et al. 2008).

Materials and methods

Experimental setup

In this work two different organic matrices were used both as fuel and microbial source for MFCs: a top soil (S) and a composted organic fertilizer (A). In April 2009, the soil was sampled from 0 to 20 cm layer of a natural soil located in the experimental field "Celimontano" of the CRA-RPS research center, Rome (Italy) (41°53′ N, 12°29′ E). It presented the

following characteristics: sandy-loam texture; sand 67%, loam 22%, and clay 11%; pH 7.9, organic matter 2.51%, total nitrogen 0.15%, ads. iron. 11.8 ppm. The commercial organic fertilizer (A) was constituted by peat 70% and sand 20% of 0.3 mm diameter, humic and fulvic acids 7%, organic nitrogen 0.8%, and organic carbon 38%, pH 5.5–6.

The experiments were conducted using two-chambered MFCs (500 ml total volume each cell) made of glass that contained graphite rods as electrodes (diameter 4 mm, length 15 cm). The bottles were connected with a glass tube through a proton exchange membrane Nafion® 117 (DuPont, USA, 2.5 cm^2 area). An external resistance of 1,000 Ω was used and the MFC voltage was manually recorded by using a multimeter and converted into current using Ohm's law (current = voltage/resistance). Current densities were normalized to the surface area of the electrodes. Noting that the aim of this study was not to optimize power generation but to analyze the alteration of different organic materials and bacterial community during the flow of current in a microbial fuel cell. Indeed the present study did not aim for high levels of energy generation but just for the selection of defined conditions that permitted a controlled comparative analysis of different microbial alteration of the organic matter.

The anode chamber was inoculated with 50 g of organic suspension (S or A) in 500 ml phosphate buffer solution (0.2 M NaH_2PO_4) at pH 7 and made homogeneous by stirring, whereas the 500 ml aqueous cathode was buffered with a HCl solution (pH 1). A sodium acetate solution (1.0 mM) was added to the anode chamber after 8 days in order to guarantee an energetic supply for anaerobic bacterial metabolism. The submerged area of the electrodes was approximately 1,100 mm^2. The solutions were autoclaved before using them. The anodic chamber was maintained in anaerobic atmosphere by gassing with nitrogen (15 ml min^{-1}). In these systems, the anode is immersed in anoxic sediment and strict anaerobic conditions are maintained. MFCs operated at room temperature of 22±3°C without added energy sources or synthetic electron-carrying mediators.

Each sampling was carried out on MFC chambers at the beginning of the experiment (S_0, A_0) and after 3 weeks with both closed circuit (S^+, A^+) and open circuit (S^-, A^-); the collected samples were characterized by both chemical than microbiological methods whereas the graphite electrodes were analyzed by scanning electron microscopy (SEM) and microbiological analysis.

The scanning electron microscopy

For scanning electron microscopy analyses, after fixation in Karnovsky solution samples of graphite anodes were washed o.n. in cacodylate-buffered 1% and then dehydrated by acetone solutions (30% to 100%) in 5 min steps. Once in 75% acetone, dehydration was performed on polylisin-covered glass slides. Samples were then observed by a JEOL JSM 5200 scanning microscope.

Microbiological analysis

The strategy adopted in this work for the molecular characterization of both uncultivable and cultivable microbial communities potentially associated to the production of electricity relies on the following sequential steps: (1) a preliminary analysis in order to check any eventual change into the microbial community structure by denaturing gradient gel electrophoresis (DGGE); (2) isolation of the cultivable fraction of bacteria by using minimal, enriched and selective media under aerobic and anaerobic conditions; (3) a preliminary characterization of the isolates via a random amplified polymorphic DNA (RAPD) analysis in order to check the presence of common strains within the community; the comparison of the RAPD haplotypes allowed to cluster them in different groups on the basis of the identity of the amplification profiles. Bacterial isolates sharing the very same RAPD profile were considered as the same strain; (4) the phylogenetic affiliation of each bacterial strain was carried out by the analysis of the 16S rRNA genes sequence amplified via PCR.

1. Denaturing gradient gel electrophoresis

   Total DNA was extracted from 0.5 g of *S* and *A* matrices by means of the Bio101 DNA extraction kit (Q-Biogene, Carlsbad, CA) and the V6-V8 region of eubacterial 16S rDNA was amplified via PCR as described by Felske et al. (1998). The DGGE analysis was then performed with the D-CODE System (Bio-Rad) on a 6% polyacrylamide gel (acrylamide/bis ratio, 37.5:1), under denaturation conditions (urea 7 M; 40% formamide with a denaturing gradient ranging from 42% to 58%); the gels were run in 1× Tris–acetate–EDTA buffer at 75 V for 16 h at 60°C and were stained with 30 ml of 1× Tris–acetate–EDTA buffer containing 3 μl of SYBR Green I (dilution, 1:10,000) for 45 min in the dark. Using fingerprinting pattern of each plot, genetic similarities of the populations in the different samples were determined by pairwise comparison of the presence and absence of bands and of the intensity of each band in different samples with Diversity Database Software (Bio-Rad). A matrix containing similarity values was obtained with the Dice coefficient. This matrix was used to construct a dendrogram according to the unweighted-pair group method, using arithmetic average (UPGMA) cluster analysis.
2. Isolation and preparation of cell lysates for DNA amplification

Culturable bacteria were extracted in saline solution (0.85% NaCl) from the solid fraction of the inoculated sediments and plated in triplicate onto Luria-Bertani (LB) medium. Plates were then incubated at 28°C for 48 h under both aerobic and anaerobic conditions. Anoxic conditions were established by anaerobic chambers supplied with catalysts (Oxoid, UK). In order to differentiate amylolytic, glucolytic, proteolitic, and total microflora as the main substrates, starch (5.0 g/L), glucose (5.0 g/L), peptone (5.0 g/L), and peptone + glucose (5.0 g/L each) were added as many substrates to PTG basal medium which is composed by (g/L): K_2HPO_4, 1.5; $MgCl_2$, 0.5; yeast extract, 0.5; trypticase, 0.3; phytone, 0.3; and cysteine–HCl, 0.5. Incubation was carried out at 30°C for 48–72 h. After recovering of plates and counting, representative colonies were streaked on nutrient glucose agar and stored at 4°C before molecular analyses.

In order to prepare the cell lysate for DNA amplification 1 ml of a liquid culture grown overnight on LB medium were resuspended in 100 μl of sterile distilled water, heated to 95°C for 10 min, and cooled on ice for 5 min.

3. Randomly amplified polymorphic DNA fingerprinting

Random amplification of DNA fragments (Williams et al. 1990) was carried out in 25-μl containing 1× Polymed buffer, 3 mM $MgCl_2$, each deoxynucleoside triphosphate at a concentration of 200 μM, 0.5 U of Polymed Polytaq (all reagents obtained from POLYMED srl, Italy) 500 ng of primer 1253 (5′ GTTTCCGCCC 3′) (Mori et al. 1999) and 2 μl of lysate cell suspension prepared as described above.

The reaction mixtures were incubated in a thermal cycler MJ Research PTC 100 Peltier Thermal Cycler (CELBIO) at 90°C for 1 min, and 95°C for 90 s. They were then subjected to 45 cycles, each consisting of incubation at 95°C for 30 s, 36°C for 1 min, and 75°C for 2 min; finally, the reactions were incubated at 75°C for 10 min and then at 60°C for 10 min, 5°C for 10 min. Reaction products were analyzed by agarose (2% *w*/*v*) gel electrophoresis in TAE buffer containing 0.5 μg/ml of ethidium bromide.

4. PCR-amplification, sequencing, and analysis of bacterial 16S rRNA genes

Two microliters of each cell lysate were used for the amplification via polymerase chain reaction (PCR). Amplification of 16S rRNA gene was performed in a total volume of 50 μl containing 1× Polymed buffer, 1.5 mM $MgCl_2$, each deoxynucleoside triphosphate at a concentration of 250 μM, and 2.0 U of Biotaq DNA polymerase (all reagents obtained from Polymed srl, Italy) and 0.6 μM of each primer [P0 5′ GAGAGTTT GATCCTGGCTCAG, and P6 5′ CTACGGCT ACCTTGTTACGA] (Grifoni et al. 1995). A primary denaturation treatment of 90 s at 95°C was performed and amplification of 16S rRNA genes was carried out for 30 cycles consisting of 30 s at 95°C, 30 s at 50°C and 1 min at 72°C, with a final extension of 10 min at 72°C. Thermal cycling was performed with a MJ Research PTC 100 Peltier Thermal Cycler (CELBIO); 10 μl of each amplification mixture were analyzed by agarose gel (0.8% *w*/*v*) electrophoresis in TAE buffer containing 0.5 μg/ml (*w*/*v*) ethidium bromide.

For sequencing, the band of interest (observed under UV, 312 nm) was excised from the gel and purified using the "QIAquick" gel extraction kit (QiAgen, Chatsworth, CA, USA) according to manufacturer's instructions. Direct sequencing was performed on both DNA strands using an ABI PRISM 310 Genetic Analyzer (Applied Biosystems) and the chemical dye-terminator (Sanger et al. 1977).

BLAST probing of the DNA databases was performed with the BLASTN option of the BLAST program (Altschul et al. 1997). The Muscle program (Edgar 2004) was used to align the 16S rRNA sequences obtained with all the type strains of the species belonging to the same genus retrieved from the Ribosomal Database Project (http://rdp.cme.msu.edu/) (Cole et al. 2009). Each alignment was checked manually, corrected, and then analyzed using the Neighbor-Joining method (Saitou and Nei 1987) according to the model of Kimura 2-parameter distances (Kimura 1980). Phylogenetic trees were constructed with the aligned sequences using MEGA 4 (Molecular Evolutionary Genetics Analysis) software (Tamura et al. 2007). The robustness of the inferred trees was evaluated by 1,000 bootstrap re-samplings.

Organic carbon fractionation and analysis

The total organic carbon content of each matrix was quantified and fractionated. The organic suspension extracted from each MFC system were decanted and filtered through filter (0.8 μm, Millipore HA type) in order to separate the liquid phase from the solid matrix. On the liquid phase the dissolved organic carbon (DOC) was determined by a C-analyzer analytic instrument (Shimadzu TOC-5050A model) whereas on the solid phase the total organic carbon was determined according to Springer and Klee (1954).

Soluble fractions of organic carbon of the solid phase were then obtained by a sequential extraction. First of all the organic matrices (S or A) contained into the MFCs, after being decanted and filtered, were dried in an oven (60°C, 24 h); then various soluble C fractions were extracted in few sequential steps, as follows:

1. Hot water extraction: the solid matrix was suspended in water (ratio 1 g solid matrix to 10 mL bi-distilled water) and shaked at 65°C for 48 h in a thermostatic Dubnoff agitator bath. Heterogeneous suspension was cooled at

room temperature and subsequently decanted and filtered, as above indicated. On the resulting liquid phase the content of total soluble organic carbon ($C_{hot\ water}$) was analytically determined as described above.

2. Cold alkaline extraction: a 0.1 M NaOH/$Na_4P_2O_7{\cdot}10H_2O$ solution was added to the newly filtered and dried solid matrix resulting after step (1) (ratio 1 g solid matrix to 10 mL basic extracting solution), degassed with N_2 for 1 min, air-tightly sealed, and shaked at 20°C for 48 h in a thermostatic Dubnoff agitator bath. Then the suspension was decanted and subsequently filtered with the same procedure described above. The liquid phase, previously degassed with N_2 for 1 min, was left in freezing, available for being further analyzed and fractionated ($C_{cold\ alkaline}$).
3. Hot alkaline extraction: the solid matrix resulting from the step (2), after being filtered again, was dried in an oven (60°C, 24 h). After drying, a 0.1 M NaOH/$Na_4P_2O_7{\cdot}10H_2O$ solution was added (ratio 1 g solid matrix/10 ml basic extracting solution), degassed with N_2 for 1 min, air-tightly sealed and left in a mechanical shake agitator (water-bath 65°C, 48 h). At the end the suspension was cooled at room temperature, and then decanted and filtered with the usual procedure. The liquid phase, previously degassed (N_2, 1 min), was left in freezing, available for being further fractionated and analyzed ($C_{hot\ alkaline}$).
4. Humic and fulvic acids separation: liquid phases resulting from steps (2) and (3) were further fractionated according to Ciavatta et al. (1990) in order to obtain humic and fulvic fractions.
5. Extracted C and C_{HA+FA} determination: the extracted organic C after each step and the C content of the humic + fulvic acids fraction (C_{HA+FA}) were determined according to Springer and Klee (1954).

Thermal analysis

The solid matrix contained into each MFC was also analyzed by differential scanning calorimeter and thermogravimetry (TG) in order to highlight possible organic matter chemical–physical transformations derived by the current production. Measures were simultaneously carried out with a Netzsch STA 409 Simultaneous Analyzer (Netzsch-Gerätebau, Selb, Germany) equipped with a TG/DSC sample carrier supporting a type S thermocouple (PtRh10-Pt). Approximately 20 mg of S or A samples, after gentle manual grinding in an agate mortar, were weighted into alumina crucible and subjected to two replicated thermal scans, at 10°C min^{-1} heating rate from ambient temperature to 800°C under static air atmosphere according to Dell'Abate et al. (2000). The Netzsch applied software SW/cp/311.01 was used for data processing. During DSC measurement, the temperature difference between sample and reference material was recorded as a direct measure of the difference in the heat-flow rates; from DSC curves peak temperature, namely the temperature at which heat flux reached the maximum, was recorded for each thermal event. In TG, the weight gain or loss (expressed as a percentage) of a sample was measured during the thermal program. The first derivative of the TG trace (DTG) represents the weight loss rate (expressed as % min^{-1}): calculation of DTG onset and peak temperatures allows for the distinction among subsequent decomposition steps. Results were expressed as the weight loss of the sample attributed to the decomposition of total organic matter in the proximate temperature range 180–600°C (Exo_{tot}), composed by the following fractions: mainly cellulosic components from about 180°C up to 410°C (Exo_1) whereas exothermal oxidation of more complex and condensed organic molecules, such as lignin and humified compounds occurs in the temperature range 410–600°C (Exo_2) (Dell'Abate et al. 2000; Flaig et al. 1975; Lopez-Capel et al. 2005). The actual starting and end reaction temperatures for each sample may vary within the broad ranges indicated before depending on the nature and complexity of reacting organic substrates.

Statistical analysis

Analysis of variance (ANOVA) was performed in order to evaluate the main effects of current production on the analyzed organic substrates (SPSS v.11). Data were tested for homogeneity of variance before performing ANOVA and then put through post-hoc test (Duncan).

Results

Electricity generation from MFCs

As expected microbial fuel cells inoculated with the fertilizer (A) generated direct electric current well above than counterparts incubated with soil (S) and the MFCs systems without any acetate addition used as control showed lower values as compared to MFCs added with it (Fig. 1). In fact the addition of acetate after 8 days significantly increased the electrochemical activity of nonsterilized soil whereas had no effect on sterilized soil (data not shown), suggesting that the electron transfer in our soil-inoculated MFCs was mediated by microbial communities under anaerobic conditions. Anodic current densities in MFCs supplied with A ranged from 372 to 481 mA/m^2 within 8 days, increased after the addition of acetate (+38.9%) and a maximum was established after 15 days (1,106 mA/m^2). Anodes from the MFCs supplied with S showed higher values in the first 8 days, decreasing from 286 to 48.6 mA/m^2 and the addition of acetate did not

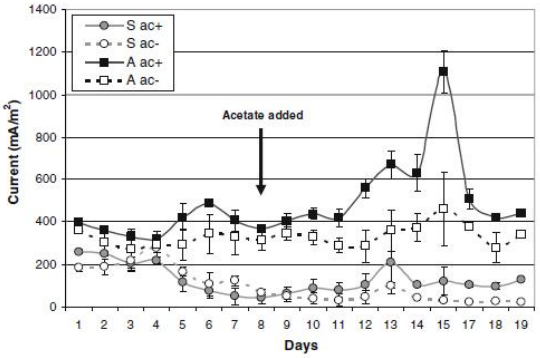

Fig. 1 Generation of electric current by microbial communities naturally present in soil and in fertilizer samples. Acetate was added after 8 days of incubation and supplied with acetate (S ac+, A ac+) or not (S ac−, A ac−). The effect of acetate supply was more evident in A than in S samples. All fuel cells were operated with 1,000 Ω load of resistance

provide any significant increase except after 13 days when a maximum current was produced (230.5 mA/m^2).

Scanning electron microscopy

The SEM analysis conducted on the surface of anodic electrodes at the end of incubation period showed a microbial biofilm on the electrode of the MFC supplied with the fertilizer with the closed circuit (A^+), whereas MFCs inoculated with soil did not show any significant biofilm layer (Fig. 2). When soil was used as inoculum the anode surface was largely characterized by irregular flakes (Fig. 2c). In contrast when the fertilizer A was used, the anode surface was more regularly shaped and

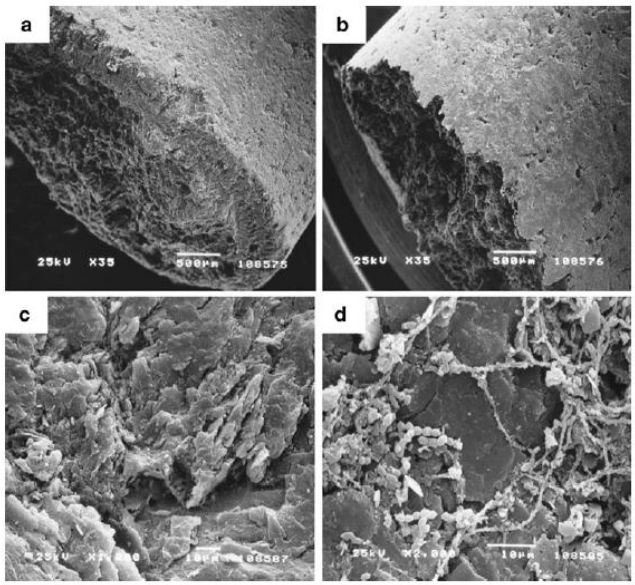

Fig. 2 Scanning electron microscopy showing imagines of the top of the anodic electrode of the MFCs inoculated with S (**a**) and A (**b**) (magnification ×35) and the particular of the surface of the electrode of the MFC added with A (**d**) (magnification ×2,000) and S (**c**) (magnification ×1,000) covered with or without microbial biofilm, respectively

an abundant biofilm featuring bacterial cells was observed (Fig. 2d).

Community analysis by DGGE

Changes in microbial communities during MFC operation were analyzed by DGGE which showed significant differences in bacterial composition of the solid phase of MFC soil suspension and fertilizer. Based on the migration distance, intensities and similarities between the lanes of the DGGE gel the banding patterns revealed the occurrence of distinctive bacterial communities at inoculation time (S_0, A_0), after 3 weeks of incubation with a closed circuit (S^+, A^+) and after 3 weeks with an open circuit (S^-, A^-), clearly showing that the bacterial communities differently changes during the incubation into the MFCs under different conditions (Fig. 3). In fact the UPGMA clustered separately bacterial communities from S^- to S^+ samples which showed similarity values below 50% whereas the similarities between S^+ and S_0 were almost 60%. UPGMA clustering showed similarity values around 40% between initial samples A_0 and samples incubated in MFCs whereas the similarities detected after 21 days of incubation in MFC systems between samples A^+ and A^- were more than 74%. In conclusion at the end of the incubation period the dominant bands of bacterial fingerprint from MFC systems with current S^+ and A^+ appeared to be significantly different from its relative no-current S^- and A^- samples and initial samples S_0 and A_0.

Isolation of bacteria

In order to achieve the microbial counting of colony forming units (CFUs), colonies were obtained from the solid fraction of S and A sampled from the anodic chambers of MFCs as described in Materials and methods section. Microbial counts were performed with a minimal medium supplied of glucose, starch, or proteinaceous compounds to evaluate some representative group of microorganisms with different metabolic properties under both aerobic and anaerobic conditions typical of natural environment and anodic MFC's chamber, respectively. Data obtained are reported in Table 1 and expressed as number of bacteria per gram of sediment.

The CFUs values obtained on enriched media showed similar results in both S and A samples regardless any current production, but significant differences were evidenced for colonies grown under both aerobic and anaerobic conditions. In fact the total amount of bacteria grown under aerobic conditions did not appear to be significantly affected neither by incubation nor by the presence of the circuit. However, the quantitative analyses of viable microflora have shown—for soil aerobic bacteria—an high variability of values obtained under experimental conditions, pointing out an increase of proteolytic microflora at the end of the incubation regardless the circuit was open or not. On the contrary proteolytic bacteria extracted from A samples did not show significant differences under aerobic conditions. At the end of incubation, the glucolytic bacteria

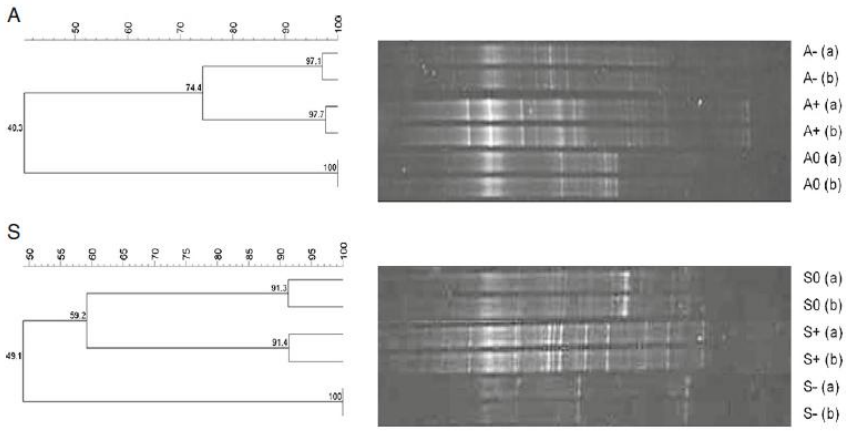

Fig. 3 16S rRNA gene DGGE profiles (V6–V8 region) of anodic eubacterial communities from soil (*S*) and fertilizer (*A*) used to inoculate the fuel cell sampled at initial time (S_0, A_0) and after 3 weeks of incubation with closed circuit (S^+, A^+) and open circuit (S^-, A^-). Scale bar numbers indicate similarities among profiles (Dice coefficient)

Table 1 Values of CFU (no. of colonies per gram) of cultivable bacteria isolated under both aerobic and anaerobic conditions from soil and fertilizer at initial time (S_0, A_0), after 3 weeks both with current (S^+, A^+) and without current (S^-, A^-)

Sample	Total	Glucolytic	Proteolytic	Amylolytic
Aerobic conditions				
S_0	3.8×10^7	9.8×10^4 a	4.9×10^5 a	3.0×10^7 a
S^+	2.1×10^7	3.0×10^5 a	1.0×10^7 b	9.7×10^2 b
S^-	2.0×10^7	5.5×10^3 b	1.5×10^7 b	4.5×10^5 c
A_0	4.7×10^7	5.1×10^4 a	6.0×10^6	3.0×10^5 a
A^+	1.5×10^7	1.0×10^4 a	1.0×10^7	6.9×10^4 b
A^-	6.4×10^7	1.5×10^7 b	7.7×10^6	6.2×10^6 c
Anaerobic conditions				
S_0	4.0×10^5	1.5×10^5	3.0×10^5	2.9×10^5 a
S^+	3.1×10^6	3.1×10^5	5.1×10^5	2.6×10^6 b
S^-	6.6×10^6	5.9×10^6	9.5×10^5	5.1×10^5 a
A_0	3.2×10^6	1.9×10^6 a	3.1×10^6 a	1.8×10^6
A^+	5.9×10^5	4.0×10^4 b	2.1×10^5 ab	5.3×10^5
A^-	3.0×10^5	5.0×10^4 b	3.9×10^4 b	2.1×10^5

For each parameter, different letter indicate significant differences (Duncan Test)

extracted from S and grown under aerobic conditions significantly increased in S^+ (3.0×10^5 CFUs g^{-1}) as compared to S^- (5.5×10^3 CFUs g^{-1}). In contrast the glucolytic bacteria isolated from A increased when the circuit was open (A^-). The amylolytic fraction extracted from both soil and the fertilizer significantly decreased when the circuit was closed (S^-, A^-) whereas an increase of the glucolytic bacteria was observed in the fertilizer samples when the circuit was open.

As far as regard anaerobic bacteria, counts were more comparable among experimental thesis but appeared generally lower than under aerobic conditions (Table 1). Furthermore S and A showed some different trends taking into consideration the quantitative evolution of microflora. For example the glucolytic fraction increased in S^- as compared to S^+ and S_0 whereas in A^+ and A^- samples the CFU's values significantly decreased as compared to the initial control A_0 regardless the circuit was connected or not. The proteolytic microflora extracted from S did not shown any significant change at the end of incubation whereas a significant decrease in bacteria extracted from the fertilizer was observed, especially in A^-. Whenever the circuit was closed, amylolytic microflora extracted from soil significantly increased as compared to S^-. In contrast no significant changes occurred in CFU values of amylolytic bacteria obtained from A.

Random amplified polymorphic DNA analysis

The RAPD fingerprinting was performed on the 48 bacterial strains isolated from the solid phase of the soil suspension and the 58 isolated from the solid phase of the A fertilizer for a total of 106 bacterial strains (Table 2). All of the bacterial strains isolated from S at the initial time grew up under aerobic conditions, whereas in A only about 53% were aerobic. At the final time, after 3 weeks of incubation the anaerobic isolates from S were 7.7% with no current and 42.8% under current producing conditions. The final anaerobic bacterial isolates from A amounted to 41.1% of the total with no-current production and 61.9% with current on when the circuit was closed.

Each of the 106 RAPD profiles was compared with each other in order to cluster bacterial isolates showing the same haplotype. In this way, 26 and 14 different haplotypes were obtained from S and A, respectively, for a total of 40 different RAPD haplotypes.

Phylogenetic affiliation of bacterial isolates

In order to affiliate a bacterial strain representative of each RAPD haplotype to a given taxon, the nucleotide sequence of the 16S rRNA gene from one representative per each RAPD group exhibiting the same profile was determined. To this purpose the 16S rRNA genes were amplified via PCR from 40 representative strains as described in Materials and Methods and an amplicon of the expected size was obtained from all strains (data not shown). Each amplicon was purified from agarose gel and the nucleotide sequence was then determined. Each of the 40 sequences obtained was used as seed to probe the nucleotide databases using the BLASTn option of the BLAST program (Altschul et al. 1997) (Table 2). The sequences of all the type strains of the species belonging to the same genus of each sequence (on the basis of the BLAST analysis results) were retrieved from the Ribosomal Database Project (http://rdp.cme.msu.edu/) (Cole et al. 2009) and aligned using the Muscle program (Edgar 2004); each alignment was then used to construct the phylogenetic trees reported in Additional file 1.

The whole data obtained from MFCs supplied with S revealed that the 26 strains were representative of six bacterial genera, four gram positive (*Arthrobacter*, *Bacillus, Lysinibacillus* and *Clostridium*) belonging to Actinobacteria and Firmicutes and two gram negative (*Pseudomonas* and *Enterobacter*) belonging to Proteobacteria. Data obtained from MFCs added with A revealed that the 14 strains were representative of three bacterial genera (*Pseudomonas*, *Enterobacter*, and *Stenotrophomonas*) belonging to γ-Proteobacteria. In particular the analysis of the phylogenetic trees revealed that:

1. The 12 isolates belonging to the genus *Arthrobacter* joined the cluster including sequences from *Aspergillus oryzae*, *Arthrobacter pascens*, and *Agromyces ramosus*.
2. Eighteen isolates were assigned to the genus *Bacillus*, with four of them clustering with *Bacillus megaterium*;

Table 2 Distribution of RAPD haplotypes obtained by bacteria isolated from MFCs under both aerobic and anaerobic conditions and their relative taxonomic classification determined by 16S rDNA sequencing

	RAPD haplotype	Representative strain	Sampling						No. of isolates/ haplotype	% of total	Next relative by GenBank alignment			
			Initial (aerobic) No current	Initial (anaerobic) No current	Final (aerobic) No current	Final (anaerobic) No current	Final (aerobic) Current	Final (anaerobic) Current			Organism	Identity (%)	Phylum or class	Accession number
Soil (S)	1	TiS_AE_1	3	0	0	0	0	0	3	6.3	*Lysinibacillus* sp. E4	99	Firmicutes	JN082733.1
	2	TiS_AE_2A	2	0	0	0	0	0	2	4.2	*Bacillus tequilensis* strain km11	99	Firmicutes	JF411301.1
	3	TiS_AE_2B	1	0	0	0	0	0	1	2.1	*Bacillus nealsonii* strain BP11_4A	99	Firmicutes	JN644556.1
	4	TiS_AE_4A	1	0	0	0	0	0	1	2.1	*Lysinibacillus* sp. EK-I66	99	Firmicutes	GU935302.1
	5	TiS_AE_5	2	0	0	0	0	0	2	4.2	*Bacillus* sp. *PDK002 16S*	99	Firmicutes	GU075851.1
	6	TiL AE3_C	9	0	0	0	0	0	9	18.8	*Pseudomonas aeruginosa* strain H51	100	Proteobacteria	EU862087.2
	7	TiS_AE_10	1	0	0	0	0	0	1	2.1	*Bacillus subtilis* strain LXB3	99	Firmicutes	GQ861468.1
	8	TiS_AE_13	1	0	0	0	0	0	1	2.1	*Lysinibacillus* sp. *EK-I66*	99	Firmicutes	GU935302.1
	9	TiS_AE_14A	3	0	0	0	0	0	3	6.3	*Bacillus subtilis* strain: GH38	99	Firmicutes	AB301009.1
	10	TiS_AE_15	2	0	0	0	0	0	2	4.2	*Arthrobacter oryzae* strain: S32118	99	Actinobacteria	AB648959.1
	11	TiS_AE_16	1	0	1	0	0	0	2	4.2	*Arthrobacter* sp. *17a-2*	99	Actinobacteria	AY561560.1
	12	TiS_AE_18	1	0	0	0	0	0	1	2.1	*Bacillus subtilis* subsp. *inaquosorum*	99	Firmicutes	HE582781.1
	13	TfS_AE_1A	0	0	2	0	0	0	2	4.2	*Bacillus* sp. *ZSA*	100	Firmicutes	EU915719.1
	14	TfS_AE_1B	0	0	1	0	0	0	1	2.1	*Bacillus* sp. *2B5G-MG-5*	100	Firmicutes	AB533783.1
	15	E_AE_15	0	0	0	0	1	0	1	2.1	*Enterobacter cloacae* strain LCR82	100	Proteobacteria	FJ976591.1
	16	TfS_AE_3B	0	0	1	0	1	0	2	4.2	*Arthrobacter oxydans* strain 1663	99	Actinobacteria	EU086792.1
	17	TfS_AE_7	0	0	1	0	0	0	1	2.1	*Arthrobacter* sp. *SC17Y*	99	Actinobacteria	AM983505.1
	18	TfS_AE_8	0	0	2	0	1	0	3	6.3	*Bacillus* sp. *SC-A5-16*	100	Firmicutes	DQ319040.1
	19	TfS_AE_9	0	0	1	0	0	0	1	2.1	*Arthrobacter oxydans* strain 1663	99	Actinobacteria	EU086792.1
	20	TfS_AE_10	0	0	2	0	0	0	2	4.2	*Bacillus megaterium* strain PEBM08010813	99	Firmicutes	FJ685764.1
	21	TfS_AE_14	0	0	1	0	0	0	1	2.1	*Arthrobacter* sp. *HTCC345*	100	Actinobacteria	AY429698.1
	22	TfS_AN_1	0	0	0	1	0	0	1	2.1	*Clostridium* sp. BXM	100	Firmicutes	JN092128.1
	23	TfS_AN_3	0	0	0	0	0	1	1	2.1	*Enterobacter cloacae* strain LCR82	100	Proteobacteria	FJ976591.1
	24	TfS_AE_11	1	0	0	0	1	0	2	4.2	*Arthrobacter* sp. *17a-2*	99	Actinobacteria	AY561560.1
	25	TfS_AE_12	0	0	1	0	0	0	1	2.1	*Arthrobacter oxydans* strain 1663	99	Actinobacteria	EU086792.1
	26	E_AN_1	0	0	0	0	0	1	1	2.1	*Enterobacter* sp. VET-7	99	Proteobacteria	EU781735.1
	Subtotal		28	0	13	1	4	2	48					

Table 2 (continued)

	RAPD haplotype	Representative strain	Sampling							No. of isolates/ haplotype	% of total	Next relative by GenBank alignment			
			Initial (aerobic) No current	Initial (anaerobic) No current	Final (aerobic) No current	Final (anaerobic) No current	Final (aerobic) Current	Final (anaerobic) Current				Organism	Identity (%)	Phylum or class	Accession number
Fertilizer (A)	24	VT AE 94	2	0	0	0	1	0	3	5.2	*Pseudomonas putida* strain XJ-2	100	Proteobacteria	HM641753.1
	25	VT AE 129	0	0	3	0	1	1	5	8.6	*Stenotrophomonas maltophilia* strain YLZZ-2	100	Proteobacteria	EU022689.1
	26	VT AN 8	0	1	0	0	0	2	3	5.2	*Enterobacter* sp. CCBAU 15488	99	Proteobacteria	DQ988938.1
	27	VT AN 15	0	2	0	0	0	3	5	8.6	*Enterobacter ludwigii* isolate PSB1	100	Proteobacteria	HQ242714.1
	28	VT AN 27	0	3	0	1	0	1	5	8.6	*Enterobacter* sp. R4M-A	99	Proteobacteria	GQ478256.1
	29	VT AN 36	0	1	0	2	0	1	4	6.9	*Enterobacter cloacae* strain Bru-1	100	Proteobacteria	HQ231214.1
	30	VT AE 155	2	0	2	0	0	0	4	6.9	*Pseudomonas geniculata* strain NFR19	99	Proteobacteria	GQ496660.1
	31	VT AE 169	1	0	1	0	1	0	3	5.2	*Pseudomonas putida* strain 32zhy	99	Proteobacteria	AM411059.1
	32	VT AE 174	3	0	0	0	0	0	3	5.2	*Pseudomonas* sp. TM7_1	99	Proteobacteria	DQ279324.1
	33	VT AE 184	1	0	1	0	1	0	3	5.2	*Pseudomonas putida* strain 32zhy	100	Proteobacteria	AM411059.1
	34	VT AE 185	1	1	1	2	4	0	9	15.5	*Stenotrophomonas maltophilia* strain MN6	100	Proteobacteria	FM213382.2
	35	VT AE 188	1	0	2	0	0	0	3	5.2	*Pseudomonas* sp. CT364	99	Proteobacteria	EU336940.2
	36	VT AN 43	0	1	0	1	0	1	3	5.2	*Enterobacter cloacae* subsp. *dissolvens* strain M354	100	Proteobacteria	HQ651837.1
	37	VT AN 51	0	0	0	1	0	4	5	8.6	*Enterobacter hormaechei* strain XJUHX-4	100	Proteobacteria	EU239467.1
	Subotal		11	9	10	7	8	13	58					
Total			39	9	23	8	12	15	106					

one with *Bacillusnealsonii* and *Bacilluscirculans*; 11 with *Bacillus amyloliquefaciens*, *Bacillus vallismortis*, *Bacillus mojavensis*, *Bacillus subtilis*, *Bacillus atrhophaeus*, and *Brevibacterium halotolerans*; and three with *Bacillus stratosphericus*, *Bacillus altitudinis*, and *Bacillus aerophilus*.

3. Five isolates belonged to the genus *Lysinibacillus*. All of them clustered with *Lysinibacillus fusiformis*.
4. The unique isolate belonging to the genus *Clostridium* clustered with *Clostridium sporogens, Clostridium putrificum*, and *Clostridium Botulinum*.
5. Nine of the 33 isolates belonging to the genus *Pseudomonas* clustered with *Pseudomonas aeruginosa*, 12 with *Pseudomonas japonica* and *Pseudomonas rhizosphaerae*, whereas the other 12 joined the cluster *with Pseudomonas reinekei*.
6. Twenty-eight strains belonged to the genus *Enterobacter* with 15 of them clustering with *Enterobacter kobei and Enterobacter ludwigii*, five with *Enterobacter nimipressuralis* and *Enterobacter amnigenus*, and eight with *Enterobacter asburiae*.

The phylogenetic tree reported on additional file 1 showed all the 16S rRNA gene sequences determined in this work and their phylogenetic affiliation. The complete list of bacterial strains analyzed in this work is shown in Table 2. All the strains isolated in this work were deposited in the National Collection COLMIA (WDCM945) (http://www.colmia.it).

Analysis of organic carbon and its fractions

The total organic carbon measured in initial solid matrices (TOC_i) was 20.5 mg/g in S and 295.0 mg/g in A. Therefore, the total amount of TOC_i in 50 g of S and A was 1,025.0 mg and 14,750.0 mg, respectively. After 21 days of incubation into the anodic chamber of MFCs, the final TOC values of the solid matrices (TOC_f) decreased to 12.8 mg/g and 13.8 mg/g in S^+ and S^-, and to 219.0 mg/g and 267.7 mg/g in A^+ and A^-, respectively (Table 3). Furthermore, the current production appeared to generally decrease the content of the dissolved organic C in equilibrium in the solution of the anodic chamber. In fact the DOC value of S^- samples was 40.1 ppm (2.01 mg in 50 g of soil) which is significantly higher than 19.2 ppm (0.96 mg in 50 g of soil) registered in S^+ samples (+108%, $p<0.05$), whereas the DOC value of A^- samples was 422.7 ppm (21.1 mg in 50 g of fertilizer) versus 152.1 ppm (7.6 mg in 50 g of fertilizer) measured in A^+ (+177%, $p<0.05$). In order to evaluate the amount of C removed during the experiment from each matrix and to estimate a possible different C consumption under closed or open circuit, a C balance mass was calculated based on the initial 50 g of S or A used in the MFC experiments. The results of carbon recovery after the MFC incubation are reported in Table 3. The results showed how the MFC experiments determined a C consumption (C_c) in both soil and amendment substrates after 3 weeks of incubation, which was higher in the MFC anodic chambers with closed circuit (S^+, A^+) than in open circuit (S^-, A^-; Table 3). The difference between the C_c values detected in the two systems (close or open circuits) was attributed to the current generation and they were estimated to be about 48.5 mg/C in soil and 2447.5 mg/C in the amendment, corresponding to 4.7% and 16.6% of the initial C content, respectively.

The sediment remained as solid residue after the experiment was subjected to a sequential chemical fractionation, based on differences in solubility in water, alkaline, and acid conditions, in order to investigate eventual modifications induced to the most stable and humified organic matter fraction by the electricity generation (Table 4). The extractable fraction of organic carbon obtained with a hot water solution ($DOC_{hot\ water}$) from both soil and amendment showed a significant decrease in A^+ (−24.7%, $p<0.05$) and S^+ (−30.1%, $p<0.05$) as compared to samples incubated under no-current conditions. Organic C extracted by alkaline solutions at 20°C or 65°C ($C_{cold\ alkaline}$ and $C_{hot\ alkaline}$, respectively) from the

Table 3 Initial and final amount of C from sediments (TOC_i and TOC_f, respectively) and solutions (DOC) used as organic fuel in the MFCs, and the relative C mass balance

	TOC_i Initial C content[a] (mg)	TOC_f Final C content[a] (mg)	DOC Solubilized C content[b] (mg)	C_r C recovery[c] (%)	C_c C consumption[d] (mg)
S^-	1,025.0	688.0	2.01	67.3	335.0
S^+	1,025.0	640.5	0.96	62.6	383.5
A^-	14,750.0	13,384.0	21.1	90.9	1,344.9
A^+	14,750.0	10,950.0	7.6	74.3	3,792.4

[a] Milligrams of carbon contained in 50 g of soil or amendments used in each MFC experiment

[b] Milligrams of carbon contained after 21 days in the phosphate buffer solution (500 mL) at the equilibrium with the solid matrix and electrodes

[c] $C_r=(TOC_f+DOC)\times 100/TOC_i$

[d] $C_c=TOC_i-(TOC_f+DOC)$

Table 4 Amounts of C fractions obtained from the MFCs sediments after the sequential extraction procedure

	$DOC_{hot\ water}$ (ppm)	$C_{cold\ alkaline}$ (mg g^{-1})	$C_{hot\ alkaline}$ (mg g^{-1})	$C_{alkaline\ tot}$ (mg g^{-1})	$C_{cold\ (ha+fa)}$ (mg g^{-1})	$C_{hot\ (ha+fa)}$ (mg g^{-1})	$C_{(ha+fa)\ tot}$ (mg g^{-1})	Humification degree[a] (%)
S^-	45.1 a	4.7 a	5.3	10.0	2.1 a	2.6 a	4.7 a	47 a
S^+	31.5 b	5.6 b	5.2	10.8	0.7 b	1.8 b	2.5 b	23 b
A^-	365.3 a	39.9 a	44.4 a	84.3 a	34.3 a	21.5 a	55.8 a	66 a
A^+	275.1 b	31.0 b	32.7 b	63.7 b	15.2 b	19.2 b	34.4 b	54 b

For each parameter, different letter indicate significant differences (Duncan Test)

[a] Relative amount of the humic and fulvic carbon present in the final solutions after sequential extraction calculated as percentage ratio of $C_{(ha+fa)}$ from cold plus hot alkaline extractions to C_{tot}

A^+ sediments at the end of the experiment was significantly lower than in A^- at both 20°C than 65°C (−22.3% and −26.1%, respectively). On the other hand sample S^+ showed the $C_{cold\ alkaline}$ values significantly higher than the relative control S^- without current (+19.1%, $p<0.5$) whereas the values of $C_{hot\ alkaline}$ obtained at 65°C were similar (Table 4).

In general, the liquid phase of samples incubated under closed-circuit conditions, such as S^+ and A^+, showed a significant decrease of the C of the humic and fulvic acids fraction ($C_{ha+fa\ tot}$). In particular the amount of C_{ha+fa} extracted at 20°C ($C_{cold\ (ha+fa)}$) from S^+ samples is significantly lower than S^- both (−66.6%, $p<0.05$) and at 65°C ($C_{hot\ (ha+fa)}$) (−30.7%, $p<0.05$). Furthermore, A^- showed $C_{cold\ ha+fa}$ values approximately double than A^+ (+125.6%, $p<0.05$) whereas $C_{hot\ (ha+fa)}$ values were also significantly higher in A^- than on A^+ samples (+11.9%, $p<0.05$).

As a selective consumption of the soluble humified fraction was observed in our experiment, especially under electricity generation (Table 4), in order to highlight chemical–physical differences in organic matter related to their stabilization level we carried out a preliminary investigation on thermal stability on the MFCs solid phases.

The results obtained by thermal analysis (TA) revealed poor qualitative shifts in the thermostability of soil organic matter fractions (200–550°C) of samples S^+ and S^-, whereas samples A^+ and A^- showed significant differences (Fig. 4). In particular, the clear two steps oxidation pattern of A^+ reveals the presence of two distinct main thermally active organic pools, which give maxima of heat flow (peaks) at about 289 and 461°C. The oxidation reactions detected by the DSC curves are associated to distinct weight losses registered as TG curve in the thermal ranges 179–312°C (Exo1, 25% of weight loss) and 312–553°C (Exo2, 14.4% weight loss), respectively. Finally sample A^- showed a thermal pattern characterized by an unique broad oxidation thermal effect in the range 200–550°C, and the associated total weight loss amounted to 43.6%, higher than the A^+ sample total weight loss.

Discussion

Although in a previous work a soil has already been used as a bacterial source for electrical production (Niessen et al. 2006), to our knowledge this is the first work in which

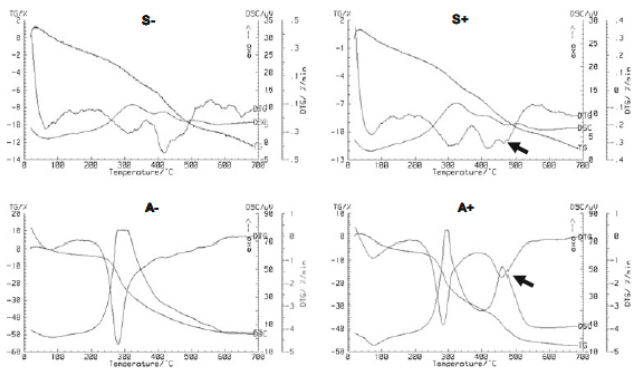

Fig. 4 Differential scanning calorimetry, thermal gravimetry, and derivative thermal gravimetry curves of soil and fertilizer from MFCs with (S^+, A^+) and without (S^-, A^-) electricity generation, respectively. They reveal qualitative shifts in the thermostability of soil organic matter fractions, including clay-associated organic matter

untreated natural top soil was used as both electroactive bacterial source and organic substrate to produce electricity without any previous bacterial inocula or mediator addition (Pant et al. 2010). Furthermore, although several sediments or complex compounds have been used as fuel in previous experiments with MFCs, however all of these substrates origin essentially from anaerobic or microaerobic environments, naturally enriched of electroactive microorganisms whereas in this work two organic matrices from aerobic environments were used. Electricity generation by MFCs supplied with a fertilizer has been previously reported by Scott and Murano (2007) but in that work the authors used a commercial manure sludge which was dried and reactivated by hydration and incubation before being used. In our case the fertilizer was directly supplied to MFCs without any preliminary treatment in order to avoid any potential alteration of endogenous microbial community.

As mentioned before, it is worth noting that in this work the MFCs systems were just used as tools to easily achieve measurable current production from two organic matrices to enrich a microbial consortium generating electricity and to study the microbial alteration of OM regardless the final power density. Nevertheless both the current density and the pattern of electricity production detected in this work were consistent to those observed by other authors who obtained microbially mediated current production using complex substrates sources or sediment MFC systems and observed a rapid increase of current production within the first days of incubation. For example the maximum current production in sediment MFCs usually ranges from 2 to 254 mA/m^2 (Holmes et al. 2004; Mathis et al. 2008; Hong et al. 2010) whereas in a number of MFCs inoculated with wastewaters the current density achieved values between 50 and 3,000 mA/m^2 (Pant et al. 2010).

In this work, patterns of current production during 21 days of incubation showed higher values for the MFCs added with A than with S. This was expected as the significant higher content of OM in A with respect to S, 2% and 30%, respectively, should have enhanced the mineralization process. According to Mathis et al. (2008), a significant increase of current production was observed after the addition of acetate, especially in A samples, whereas a lower effect was detected in MFCs incubated with S (Fig. 1). This could be due to the low amount of labile and low-molecular weight OM available for soil microbial communities which operate under anaerobic conditions. It could be also coherent with the great difference of initial content of OM in A and S samples, and it could even have conditioned the biofilm development as well. In fact the SEM analysis showed a clear development of a microbial biofilm on the surface of the anodic electrode in MFCs incubated with A but not with S. Furthermore, usually a longer incubation period is needed to make the biofilm to be developed, as showed by Kim et al. (2004). On the other hand the initial microorganism associated to the organic substrate and the chemical–physical properties of the matrix could also be responsible of such result. However, the rapid increase of the current production observed after the addition of acetate was not immediate. The reason of such delayed increase in current production is unclear. It could be related to the low acetate concentration we used in this work (1 mM), in order to guarantee a minimum of energy source in the MFC systems, as compared to other similar studies which showed an immediate increase of current production after the addition of 5 mM sodium acetate (Lee et al. 2003) or 25 mM (Mathis et al. 2008). However, such studies used a continuous flow MFC system inoculated with activated sludge or a batch mode MFC inoculated with marine sediment and replaced with acetate whereas in our case the added acetate represents just a little fraction of the organic molecules already available in the system. Therefore the acetate might have not been immediately used by the exoelectrogenic microbial community which, indeed, could have chosen other substrates as alternative C-source under anaerobic conditions. Moreover, it is also likely that acetate is depleted by nonexoelectrogenic bacteria present in the system, thus not providing any direct current production.

As expected the DGGE analysis showed a significant change of bacterial community structure under current or no-current producing conditions, clearly showing that the bacteria had been enriched during the operation of the MFC, according to most of the known literature (Kim et al. 2004; Rabeay et al. 2004, 2007; Aelterman et al. 2006). However, it was quite surprising to detect such changes after a so short period in A but also in S samples. In fact it is possible to observe that just 21 days of incubation were enough to significantly modify the composition of bacterial species. At the initial time of incubation (S_0, A_0) the DGGE fingerprint evidenced two different bacterial communities indigenous to A and S which were differently selected by current production after 21 days. This result confirmed that exoelectrogenic communities are strictly dependent on the energy source as previously showed by other authors (i.e., Choo et al. 2006). Furthermore, both the effect of the incubation into the chamber and the electrogenic enrichment due to the internal conditions of the MFC system was observed, suggesting that the bacterial consortia is not stable with time regardless the current production.

As the microbial communities selected into current-producing MFCs are supposed to be directly or indirectly involved in the electrogenic process, we focused our attention of the culturable fraction in order to isolate and subsequently analyze any electroactive bacteria. The use of elective media allowed us to discriminate among microbial populations characterized by capabilities to degrade different organic substrates under aerobic and anaerobic

conditions. Interestingly, glucolytic bacteria extracted from A and S samples and grown under aerobic conditions showed opposite response depending on the current. In fact the CFU values of glucolytic bacteria obtained from S^- samples decreased as compared to S_0 and S^+ whereas glucolytic bacteria extracted from A^- showed CFU values significantly higher than in A_0 and A^+. In contrast no significant differences were detected in glucolytic bacteria grown under anaerobic conditions, regardless the current production. This different behavior observed under aerobic conditions appeared to be also related to the amylolytic activity which showed a strong decrease of CFU values in S^+ and A^+. Such data indicates that at the end of incubation the MFCs under current-producing conditions selected more for glucolytic than amylolytic bacteria, especially in S aerobic samples, suggesting that the electrogenic process in MFC inoculated with S could be more likely induced by labile organic compound (i.e., carbohydrates) consumption rather than complex and recalcitrant organic substrates. In contrast the electricity producing MFCs appeared to reduce both glucolytic and amylolytic bacteria from samples A suggesting different metabolic pathways for OM degradation. The soil proteolytic bacteria did not generally appear to be affected by current production and this evidence suggests a scarce role of the protein fraction of OM in the electrogenic process. In general these results confirm that the available OM and its quality are crucial for microbial selection. These data also suggested that such populations can be considered autochthonous and that a selective approach based on the available substrate was effective for the isolation of a large number of strains, implying the possibility to further investigate for the presence of potential exoelectrogenic bacteria.

The detection of several RAPD haplotypes revealed a high degree of biodiversity at the strain level. However, the RAPD analysis also revealed that several isolates exhibited very similar profiles suggesting that they might belong to the same species or genus and in some cases different isolates shared the same profile, strongly suggesting that they actually represent the same strain.

Several authors have found members of Proteobacteria in MFCs (Kim et al. 2004; Aelterman et al. 2006). Our findings confirm these results as most of the isolates obtained in this study were closely related to Proteobacteria, especially in MFCs incubated with A where the 100% of the isolates belonged to this class. The most abundant bacterial species present in S samples at the end of the incubation under current-producing conditions were *Enterobacter* sp. and *Bacillus* sp. which are well known to be involved in electrogenic processes like observed in other works (Rabeay et al. 2004; Lovley 2008) but also fermenters such as *Arthrobacter* sp. and *Clostridium* sp. which have been also detected in other studies (Morris et al. 2009). Their presence induces to suppose that synergistic interactions among microbes might be an influential factor to degrade complex substrates in MFCs. It is known that some bacterial species, such as *P. aeruginosa*, can produce compounds like phenazine and pyocyanin that function as electron shuttles between the bacterium and an electron acceptor (Rabaey et al. 2005). This kind of electron transfer does not need any direct contact between bacteria and electrode and it could explain the absence of a microbial biofilm on the anodic electrode surface MFCs added with S. However, *P. aeruginosa* appeared to be poorly correlated to electrogenic processes as it was not detected in samples incubated under current-producing conditions, whereas *Enterobacter cloacae*, *Arthrobacter* sp. and *Bacillus* sp. were present. However, as the electrogenic mechanism is an essentially anaerobic process, the putative bacterial species involved in the current-producing reactions appeared to mainly belong to *Enterobacter* sp. and *E. cloacae*. *Stenotrophomonas maltophilia*, capable of nitrate reduction and already found as dominant on MFC's anodes (Morris et al. 2009), was the most abundant species in A samples under current-producing conditions. This result suggests that the final electron acceptor could be other than the anode electrode such as nitrate or molecules with electron potential close to that of nitrate. Thus denitrification could be a putative metabolic pathway for organic waste degradation at the anode of an MFC. Although *E. ludwigii* and *Enterobacter hormaechei* species appeared to be also dominant under anaerobic conditions, their electrogenic properties have still to be directly addressed.

The chemical analysis showed a significant decrease of TOC_f and DOC values in the closed-circuit MFCs indicating that the production of electricity either increased the consumption (C_c) of the available OM of the fuel sources provided to the MFC systems, in according to other authors who made similar observations with marine sediments (Hong et al. 2010) and sewage sludge (Jiang et al. 2010). The C_c attributed to the current generation in soil and fertilizer (4.7% and 16.6% of the initial C content, respectively) could be also related to the microbial secondary metabolism. For example the generation of methane and CO_2 cannot be excluded, as previously reported (Hong et al. 2010). In fact in a microbial fuel cell bacteria have limited options for their final electron acceptor and they can either use the electrode or produce reduced metabolites, such as methane or hydrogen gas, which have not been measured in this work. Furthermore, the diversity of bacterial grow rate is also important to explain both the different C_c values and the lack of correlation between C_c and bacterial CFUs could be due to the contribution of uncultured organisms in the degradation of OM.

It was also observed that the extent of C_c in the anodic chamber of MFCs depended not only on the different

quantity but also on the qualitative characteristics of organic substrates, as shown by the selective consumption of the soluble humified fraction detected in our experiment, especially under electricity generation (Table 4). This is in accordance with Hong et al. (2010) who reported both quantitative and qualitative changes of organic matter in marine sediments during electricity generation. In that study the authors observed an enhanced humification process under closed-circuit conditions but this result was not confirmed by the fractionation analysis of soluble C obtained from the solid phases which showed that humic substances decreased when electrical current was produced, as confirmed by higher $C_{cold\ (ha+fa)}$, $C_{hot\ (ha+fa)}$ and the humification degree values detected in MFCs under current-producing conditions. This is a very interesting result because humic substances are known to be a suitable electron donor and an energy source for the assimilation of carbon from alternative sources such as nitrate or fumarate (Coates et al. 1998, 2002). As humic substances are considered not biodegradable as a carbon source (Coates et al. 2002), the results of the present study are more likely due to a decreased solubility of humic fraction of OM at the end of incubation, than to their degradation humic substances used as suitable C-source. Furthermore, most of Proteobacteria are also known for their ability to oxidize complex organic and humic compounds (Coates et al. 2002) and it could explain the significant alteration of humic substances within MFCs inoculated with both S and A. Such hypothesis is supported by thermal analysis which evidenced the formation of a chemical–physical more stable conformation of the OM after electricity generation, especially in A samples, suggesting that bacterial activity stimulated OM oxidation towards a globally more stabilized form, similar to that occurring during aerobic composting processes. In fact the presence of the two peaks of oxidation pattern in A^+ which give maxima of heat flow at about 289 and 461°C is typical of stable and humified organic matter, since the first peak is commonly referred to exothermic decomposition of the most thermo-labile organic compounds, characterized by the presence of aliphatic and carboxylic groups, and the second one, thermally more stable and energetic, to exothermic oxidation of molecules containing aromatic moieties (Flaig et al. 1975; Leinweber and Schulten 1999). Furthermore the value of the ratio Exo2/Exo1 indicates that the material reached a good level of stabilization in comparison with other compost previously investigated (Dell'Abate et al. 2000; Klammer et al. 2008). In fact the ratio between the weight losses associated with the second and the first exothermal reactions (R1=Exo2/Exo1) is a thermal stability index representing the relative amount of the thermally more stable organic matter fraction with respect to the less stable one, regardless of either sample moisture level or ash content (Dell'Abate et al. 2000; Klammer et al. 2008). On the contrary, sample A^- showed a thermal pattern characterized by a unique broad oxidation thermal effect in the range 200–550°C, typical of scarce mature compost. This confirms the data discussed above on the consumption of organic carbon due to the current generation and the hypothesis of humification stimulation under closed-circuit conditions (Hong et al. 2010). Moreover, if a selective activity of bacterial communities occurs under closed or open circuit as consequence of electricity generation, it should not be surprising that the different thermal patterns were found in A^+ and A^-, since in a previous investigation on a number of compost of different origins a correlation was found between the thermal stability indices and the bacterial community patterns (Klammer et al. 2008). On the other hand, the thermograms of S samples from MFCs are not much explicative, possibly due to the much lower amount of organic matter involved, thus it should be speculative, at this stage, try to find an explanation of the little more distinct DTG peak at about 470°C observed in S^+ samples and indicated by the arrow in Fig. 4.

In conclusion, our results demonstrated that electroactive bacteria are commonly present even in aerobic organic substrates such as soil or a fertilizer and that MFCs could represent a powerful tool for exploring the mineralization and humification processes of their OM. In fact the observed changes in OM properties were analogous to those commonly observed in the early stages of the soil OM diagenetic process (i.e., humification). Such a humification-like process was evidently more stimulated when electrical current was produced than under no-current conditions with the simultaneous increase of Proteobacteria. Therefore, it is possible to suppose that Proteobacteria are directly or indirectly involved in the current generation and that electroactive organisms play an important role even in the turnover of the organic matter of soil environments. For example *Enterobacter* sp., which appeared to be one of the most involved species in the electrogenic processes, could be responsible of humification-like process of OM as well. Further efforts will be also focused on the putative remediation capacities of such bacteria. In fact the potential application of anodic MFC technology for enhancing direct anaerobic biodegradation of polluted environments (Morris et al. 2009) could also represent a low-cost alternative to electrokinetic approaches commonly used for soil remediation (Virkutyte et al. 2002). Emerging questions are: (1) which is the entire fraction of soil bacteria with electrogenic potential? (2) What is the role of other bacteria in relation to exoelectrogenic strains in anodic communities, and how do mixtures of communities affect power production and OM oxidation? Answering these questions will provide useful insights into the ecology of soil and complex functions within exoelectrogenic microbial communities.

Acknowledgments This research was supported with funds from the Italian Ministry of Agricultural, Food, and Forestry Policies (MIPAAF) and it is part of the results of the BEM project (D.M. 247/07).

References

Aelterman P, Rabaey K, Pham HT, Boon N, Verstraete W (2006) Continuous electricity generation at high voltages and currents using stacked microbial fuel cells. Environ Sci Tech 40:3388–3394

Altschul SF, Madden TL, Schäffer AA, Zhang J, Zhang Z, Miller W, Lipman DJ (1997) Gapped BLAST and PSI-BLAST: a new generation of protein database search programs. Nucleic Acid Res 25:3389–3402

Bond DR, Lovley DR (2003) Electricity production by *Geobacter sulfurreducens* attached to electrodes. Appl Environ Microbiol 69:1548–1555

Bond DR, Holmes DE, Tender LM, Lovley DR (2002) Electrode-reducing microorganisms that harvest energy from marine sediments. Science 295:483–485

Brüchert V, Arnosti C (2003) Anaerobic carbon transformation: experimental studies with flow-through cells. Mar Chem 80:171–183

Choo YF, Lee J, Chang IS, Kim BH (2006) Bacterial communities in microbial fuel cells enriched with high concentrations of glucose and glutamate. J Microbiol Biotechnol 16(9):1481–1484

Ciavatta C, Govi M, Vittori Antisari L, Sequi P (1990) Characterization of humified compounds by extraction and fractionation on solid polyvinylpyrrolidone. J Chromatogr 509:141–146

Coates JD, Ellis DJ, Blunt-Harris EL, Gaw CV, Roden EE, Lovley DR (1998) Recovery of humic-reducing bacteria from a diversity of environments. Appl Environ Microbiol 64(4):1504–1509

Coates JD, Cole KA, Chakraborty R, O'Connor SM, Achenbach LA (2002) Diversity and ubiquity of bacteria capable of utilizing humic substances as electron donors for anaerobic respiration. Appl Environ Microbiol 68(5):2445–2452

Cole JR, Wang Q, Cardenas E, Fish J, Chai B, Farris RJ, Kulam-Syed-Mohideen AS, McGarrell DM, Marsh T, Garrity GM, Tiedje J (2009) The ribosomal database project: improved alignments and new tools for rRNA analysis. Nucleic Acids Res 37:D141–D145

De Schamphelaire L, van Den Bossche V, Dang HS, Höfte M, Boon N, Rabaey K, Verstraete W (2008) Microbial fuel cells generating electricity from rhizodeposits of rice plants. Environ Sci Technol 42:3053–3058

Dell'Abate MT, Benedetti A, Sequi P (2000) Thermal methods of organic matter maturation monitoring during a composting process. J Therm Anal Calorim 61:389–396

Edgar RC (2004) MUSCLE: a multiple sequence alignment method with reduced time and space complexity. BMC Bioinforma 5:113

Felske A, Wolterink A, Van Lis R, Akkermans ADL (1998) Phylogeny of the main bacterial 16S rRNA sequences in Drentse A grassland soils (The Netherlands). Appl Environ Microbiol 64:871–879

Flaig W, Beutelspacher H, Rietz E (1975) Chemical composition and physical properties of humic substances. In: Gieseking JE (ed) Soil components, vol. 1. Springer, Berlin, pp 119–126

Grifoni A, Bazzicalupo M, Di Serio C, Fancelli S, Fani R (1995) Identification of *Azospirillum* strains by restriction fragment length polymorphism of the 16S rDNA and of the histidine operon. FEMS Microbiol Lett 127:85–91

Holmes DE, Bond DR, O'Neill RA, Reimers CE, Tender LR, Lovley DR (2004) Microbial communities associated with electrodes harvesting electricity from a variety of aquatic sediments. Microb Ecol 48:178–190

Hong SW, Kim HS, Chung TH (2010) Alteration of sediment organic matter in sediment microbial fuel cells. Environ Pollut 158:185–191

Ishii S, Shimoyama T, Hotta Y, Watanabe K (2008) Characterization of a filamentous biofilm community established in a cellulose-fed microbial fuel cell. BMC Microbiol 8:6

Jiang J, Zhao Q, Wei L, Wang K (2010) Extracellular biological organic matters in microbial fuel cell using sewage sludge as fuel. Water Res 44:2163–2170

Kim BH, Park HS, Kim HJ, Kim GT, Chang IS, Lee J, Phung NT (2004) Enrichment of microbial community generating electricity using a fuel-cell-type electrochemical cell. Appl Microbiol Biotechnol 63:672–681

Kim GT, Webster G, Wimpenny JWT, Kim BH, Kim HJ, Weightman AJ (2006) Bacterial community structure, compartmentalization and activity in microbial fuel cells. J Appl Microbiol 101:698–710

Kim BH, Chang IS, Gadd GM (2007a) Challenges in microbial fuel cell development and operation. Appl Microbiol Biotechnol 76:485–494

Kim JR, Jung S, Regan JM, Logan BE (2007b) Electricity generation and microbial community analysis of alcohol powered microbial fuel cells. Bioresour Technol 98:2568–2577

Kimura MA (1980) Simple method for estimating evolutionary rate of base substitutions through comparative studies of nucleotide sequences. J Mol Evol 16:11–120

Klammer S, Knapp B, Insam H, Dell'Abate MT, Ros M (2008) Bacterial community patterns and thermal analyses of composts of various origins. Waste Manag Res 26:173–187

Lee J, Phung NT, Chang IS, Kim BH, Sung HC (2003) Use of acetate for enrichment of electrochemically active microorganisms and their 16S rDNA analyses. FEMS Microbiol Lett 223:185–191

Leinweber P, Schulten HR (1999) Advances in analytical pyrolysis of soil organic matter. J Anal Appl Pyrol 49:359–383

Liu H, Ramnarayanan R, Logan B (2004) Production of electricity during wastewater treatment using a single chamber microbial fuel cell. Environ Sci Technol 38:2281–2285

Lluch AV, Felipe AM, Greus AR, Cadenato A, Ramis X, Salla JM, Morancho JM (2005) Thermal analysis characterization of the degradation of biodegradable starch blends in soil. J Appl Polym Sci 96:358–371

Logan BE (2009) Exoelectrogenic bacteria that power microbial fuel cells. Nat Rev Microbiol 7:375–381

Logan BE (2010) Scaling up microbial fuel cells and other bioelectrochemical systems. Appl Microbiol Biotechnol 85:1665–1671

Logan BE, Regan JM (2006a) Microbial fuel cells—challenges and applications. Environ Sci Technol 1:5172–5180

Logan BE, Regan JM (2006b) Electricity-producing bacterial communities in microbial fuel cells. Trends Microbiol 14(12):512–518

Logan BE, Murano C, Scott K, Gray ND, Head IM (2005) Electricity generation from cysteine in a microbial fuel cell. Water Res 39:942–952

Lopez-Capel E, Sohi SP, Gaunt JL, Manning DAC (2005) Use of thermogravimetry-differential scanning calorimetry to characterize modelable soil organic matter fractions. Soil Sci Soc Am J 68:136–140

Lovley DR (2008) The microbe electric: conversion of organic matter to electricity. Curr Opin Biotechnol 19:1–8

Mathis BJ, Marshall CW, Milliken CE, Makkar RS, Creager SE, May HD (2008) Electricity generation by thermophilic microorganisms from marine sediment. Appl Microbiol Biotechnol 78:147–155

Min B, Kim J, Oha S, Regana JM, Logan BE (2005) Electricity generation from swine wastewater using microbial fuel cells. Water Res 39:4961–4968

Mori E, Lio' P, Daly S, Damiani G, Perito B, Fani R (1999) Molecular nature of RAPD markers amplified from *Haemophilus influenzae* Rd genome. Res Microbiol 150:83–93

Morris JM, Jin S, Crimi B, Pruden A (2009) Microbial fuel cell in enhancing anaerobic biodegradation of diesel. Chem Eng J 146:161–167

Niessen J, Schroder U, Scholz F (2004) Exploiting complex carbohydrates for microbial electricity generation—a bacterial fuel cell operating on starch. Electrochem Commun 6:955–958

Niessen J, Harnisch F, Rosenbaum M, Schroder U, Scholz F (2006) Heat treated soil as convenient and versatile source of bacterial communities for microbial electricity generation. Electrochem Commun 8:869–873

Pant D, Van Bogaert G, Diels L, Vanbroekhoven K (2010) A review of the substrates used in microbial fuel cells (MFCs) for sustainable energy production. Bioresource Technol 101:1533–1543

Phung NT, Lee J, Kang KH, Chang IS, Gadd GM, Kim BH (2004) Analysis of microbial diversity in oligotrophic microbial fuel cells using 16S rDNA sequences. FEMS Microbiol Lett 233:77–82

Rabaey K, Boon N, Höfte M, Verstraete W (2005) Microbial phenazine production enhances electron transfer in biofuel cells. Environ Sci Technol 39:3401–3408

Rabaey K, Rodríguez J, Blackall LL, Keller J, Gross P, Batstone D, Verstraete W, Nealson KH (2007) Microbial ecology meets electrochemistry: electricity-driven and driving communities. ISME J 1:9–18

Rabeay K, Vestraete W (2005) Microbial fuel cells: novel biotechnology for energy generation. Trends Biotechnol 23(6):291–298

Rabeay K, Boon N, Siciliano SD, Verhaege M, Verstraete W (2004) Biofuel cells select for microbial consortia that self-mediate electron transfer. Appl Environ Microbiol 70(9):5373–5382

Reimers CE, Tender LM, Fertig S, Wang W (2001) Harvesting energy from the marine sediment–water interface. Environ Sci Technol 35:192–195

Reimers CE, Stecher HA III, Westall JC, Alleau Y, Howell KA, Soule L, White HK, Girguis PR (2007) Substrate degradation kinetics, microbial diversity and current efficiency of microbial fuel cells supplied with marine plankton. Appl Environ Microbiol 73 (21):7029–7040

Rismani-Yazdi H, Christy AD, Dehority BA, Morrison M, Yu Z, Tuovinen OH (2007) Electricity generation from cellulose by rumen microorganisms in microbial fuel cells. Biotechnol Bioeng 97:1398–1407

Saitou N, Nei M (1987) The neighbor-joining method: a new method for reconstructing phylogenetic trees. Mol Biol Evol 4:406–425

Sanger F, Nicklen S, Coulson AR (1977) DNA sequencing with chain terminating inhibitors. Proc Natl Acad Sci USA 74:5463–5467

Scott K, Murano C (2007) A study of a microbial fuel cell battery using manure sludge waste. J Chem Technol Biotechnol 82:809–817

Sleator RD, Shortall C, Hill C (2008) Metagenomics. Lett Appl Microbiol 47:361–366

Springer U, Klee J (1954) Prüfung der Leistungsfähigkeit von einigen wichtigeren Verfahren zur Bestimmung des Kohlemstoffs mittels Chromschwefelsäure sowie Vorschlag einer neuen Schnellmethode. Z Pflanzenernähr Dang Bodenk 64:1

Tamura K, Dudley J, Nei M, Kumar S (2007) MEGA4: Molecular Evolutionary Genetics Analysis (MEGA) software version 4.0. Mol Biol Evol 24:1596–1599

Tender LM, Reimers CE, Stecher HA III, Holmes DE, Bond DR, Lowy DA, Pilobello K, Fertig SJ, Lovley DR (2002) Harnessing microbially generated power on the seafloor. Nat Biotechnol 20:821–825

Virkutyte J, Sillanpää M, Latostenmaa P (2002) Electrokinetic soil remediation—critical overview. Sci Total Environ 289(1–3):97–121

Williams JGK, Kubelik AR, Livak KJ, Rafalski JA, Tingey SV (1990) DNA polymorphisms amplified by arbitrary primers are useful as genetic markers. Nucleic Acid Res 18:6531–6535

Zhang Y, Min B, Huang L, Angelidaki I (2009) Generation of electricity and analysis of microbial communities in wheat straw biomasses-powered microbial fuel cells. Appl Environ Microbiol 75(11):3389–3395

Zuo Y, Maness PC, Logan BE (2006) Electricity production from steam-exploded corn stover biomass. Energy Fuel 20:1716–1721

DprE1, a new taxonomic marker in Mycobacteria

The second project on which I worked during the PhD period, was carried out in collaboration with the research group of Prof.ssa Giovanna Riccardi at the University of Pavia, and concerned the possible use of DprE1 protein as a new taxonomic marker in mycobacteria.

The *Mycobacterium* genus includes more than 50 species that have been recognized as potential human pathogens, among which the species belonging to the *Mycobacterium tuberculosis* complex (MTBC) are the most known and include human pathogens and animal-adapted pathogens (Bouakaze *et al.*, 2011). The *Mycobacterium avium–intracellulare* complex (MAC) is another important group responsible for opportunistic infections in immunocompromised individuals (Field & Cowie, 2006), while *Mycobacterium leprae* persists in developing countries, and it is the causative agent of leprosy (Suzuki *et al.*, 2012).

The interspecies genetic similarity in this genus ranges from 94% to 100%, and for some mycobacterial species, this value is higher than in other bacteria (Devulder *et al.*, 2005). In addition to the 16S rRNA gene, alternative phylogenetic markers have been proposed for mycobacteria, such as *hsp65*, *recA, sodA*, and *rpoB* genes (Adekambi & Drancourt, 2004); however no gene amplification is obtained for a few species and some closely related species are difficult to differentiate, like those belonging to MTBC complex (Mignard & Flandrois, 2007). Also multigene sequence analysis was applied to mycobacteria, for example the concatenation of four genes (16S rRNA gene, *hsp65*, *rpoB*, and *sodA*) provided a good tool of increasing the robustness of the final tree, but presented some inaccuracies, especially for MTBC complex (Devulder et al., 2005)

The essential gene *dprE1* encodes the target of five new antitubercular agents, including the benzothiazinones (BTZs) (Makarov *et al.*, 2009, Christophe *et al.*, 2009, Magnet *et al.*, 2010, Stanley *et al.*, 2012, Wang *et al.*, 2013). The DprE1 enzyme works in concert with DprE2, and it is involved in the biosynthesis of

arabinogalactan, an essential component of the mycobacterial cell wall core (Wolucka, 2008). Point mutations responsible for the substitution of Cys387 residue of *M. tuberculosis* DprE1 are responsible for BTZ resistance and this cysteine residue is highly conserved in orthologous DprE1 proteins from various BTZ-susceptible Actinobacteria; on the other site, in *Mycobacterium avium* and in *Mycobacterium aurum* that are naturally resistance to BTZ, the Cys387 residue is replaced by serine or alanine, respectively (Makarov et al., 2009). Beside BTZs, other three molecules, DNB1, VI‑9376, and 377790, have been published to form covalent bonds with the cysteine residue within the active site of DprE1, thus blocking the enzymatic activity (Christophe et al., 2009, Makarov et al., 2009, Magnet et al., 2010, Stanley et al., 2012). Until now, only one DprE1 inhibitor is able to form a noncovalent binding with Cys387 (Wang et al., 2013).

In this work 73 DprE1 amino acid sequences belonging to different *Mycobacterium* species were analyzed, revealing a high degree of sequence conservation between them. In particular the degree of conservation of twelve residues located into the DprE1 active site were evaluated and eleven of these residues are conserved in all analyzed sequences; the only exception is represented by Cys387 (position referred to *M. tuberculosis*) that, in some sequences, is replaced by an alanine.

The multialignment of these 73 amino acid sequences was used to build a neighbor-joining tree, supported by high bootstrap values showing that different strains of the same species shared a high degree of sequence similarity and were clustered together. Moreover, each species is clearly separated from the others. Therefore, DprE1 could be used as a taxonomic marker for identifying/clustering strains belonging to the same mycobacterial species.

Another interesting feature of the DprE1 phylogenetic analysis is related to the BTZ sensitivity/resistance of mycobacterial strains. Indeed, the Dpre1 tree is divided into two main clusters, each of which including mycobacterial species having Cys or Ala in position 387. On the basis of the available data, strains included in cluster

with Ala in position 387, might be susceptible to BTZs as well as to the other three DprE1 inhibitors, and actually several species susceptible to BTZs are included in this cluster. The second cluster (exhibiting an Ala387) embedded species whose representatives might be resistant to BTZs. Also in this case, some species tested to be resistant to BTZs fall into this cluster.

Finallly, a phylogenetic tree was constructed on the basis of the alignment of the concatenated amino acid sequences of the products of nine housekeeping genes from 46 *Mycobacterium* strains, to evaluate if there is a congruence between DprE1 tree and the overall *Mycobacterium* phylogeny. The analysis of the concatamer tree revealed that strains belonging to the same species were clustered together, whereas different species are clearly separated, with nodes supported by very high bootstrap values (99–100%). Both the robust topology and high bootstraps suggest that the concatamer tree is much more reliable of other trees constructed using single genes. Moreover, there is no a separation between the mycobacterial BTZ-susceptible and BTZ-resistant species. Consequently, this parameter is not linked to the phylogeny of mycobacteria.

In conclusion, the whole body of data obtained suggested that DprE1 tree might represent an additional good taxonomic marker for the assignment of a mycobacterial isolate to a given species. In addition, the same marker might also give insights into sensitivity/resistanec of mycobacterial isolates to BTZs and to other drugs hitting DprE1 enzyme, simply checking for the presence/absence in position 387 of Cys residue, respectively. Lastly, the phylogenetic tree, constructed using a concatamer of nine housekeeping genes, was supported by very high bootstrap values. Consequently, this tree represents a good reference phylogeny for the *Mycobacterium* genus.

FEMS MICROBIOLOGY LETTERS

RESEARCH LETTER

DprE1, a new taxonomic marker in mycobacteria

Maria Loreto Incandela[1], Elena Perrin[2], Marco Fondi[2], Ana Luisa de Jesus Lopes Ribeiro[1], Giorgia Mori[1], Alessia Moiana[3], Maurizio Gramegna[3], Renato Fani[2], Giovanna Riccardi[1] & Maria Rosalia Pasca[1]

[1]Department of Biology and Biotechnology "Lazzaro Spallanzani", University of Pavia, Pavia, Italy; [2]Department of Biology, University of Florence, Florence, Italy; and [3]Sentinel CH, Milan, Italy

Correspondence: Maria Rosalia Pasca, Department of Biology and Biotechnology "Lazzaro Spallanzani", University of Pavia, via Ferrata 1, 27100 Pavia, Italy.
Tel.: +39 0382 985578;
fax: +39 0382 528496;
e-mail: mariarosalia.pasca@unipv.it

Received 26 July 2013; revised 23 August 2013; accepted 27 August 2013.

DOI: 10.1111/1574-6968.12246

Editor: Roger Buxton

Keywords
Taxonomy; *Mycobacterium tuberculosis*; benzothiazinones; concatamer.

Abstract

Among the species of the *Mycobacterium* genus, more than 50 have been recognized as human pathogens. In spite of the different diseases caused by mycobacteria, the interspecies genetic similarity ranges from 94% to 100%, and for some species, this value is higher than in other bacteria. Consequently, it is important to understand the relationships existing among mycobacterial species. In this context, the possibility to use *Mycobacterium tuberculosis dprE1* gene as new phylogenetic/taxonomic marker has been explored. The *dprE1* gene codes for the target of benzothiazinones, belonging to a very promising class of antitubercular drugs. Mutations in cysteine 387 of DprE1 are responsible for benzothiazinone resistance. The DprE1 tree, obtained with 73 amino acid sequences of mycobacterial species, revealed that concerning the benzothiazinone sensitivity/resistance, it is possible to discriminate two clusters. To validate it, a concatamer obtained from the amino acid sequences of nine mycobacterial housekeeping genes was performed. The concatamer revealed that there is no separation between the benzothiazinone-susceptible and benzothiazinone-resistant species; consequently, this parameter is not linked to the phylogeny. *DprE1* tree might represent a good taxonomic marker for the assignment of a mycobacterial isolate to a species. Moreover, the concatamer represents a good reference phylogeny for the *Mycobacterium* genus.

Introduction

The *Mycobacterium* genus includes several medically important species that constitute an alarming toll in human mortality. Among the species of the *Mycobacterium* genus, more than 50 have been recognized as potential human pathogens.

The species belonging to the *Mycobacterium tuberculosis* complex (MTBC) are the most known and include the human pathogens *M. tuberculosis*, *Mycobacterium africanum*, and *Mycobacterium canettii* and the animal-adapted pathogens *Mycobacterium bovis*, *Mycobacterium microti*, *Mycobacterium caprae*, and *Mycobacterium pinnipedii* as well as the recently discovered species *Mycobacterium mungi* (Bouakaze *et al.*, 2011).

Mycobacterium avium–intracellulare complex (MAC) is another important group including nontuberculous mycobacteria responsible for opportunistic infections in immunocompromised individuals (Field & Cowie, 2006), while the unculturable *Mycobacterium leprae* persists in developing countries, and it is the causative agent of leprosy (Suzuki *et al.*, 2012).

In spite of the different diseases that can be caused by mycobacteria, the interspecies genetic similarity ranges from 94% to 100%, and for some mycobacterial species, this value is higher than in other bacteria (Devulder *et al.*, 2005). Therefore, further analysis would be important to improve our understanding of mycobacterial taxonomic identity, in the context of evolution and speciation.

Even though the 16S rRNA gene is the most used molecular marker for phylogenetic analysis in bacteria, alternative markers have been proposed for mycobacteria, such as *hsp65*, *recA*, *sodA*, and *rpoB* genes (Adékambi & Drancourt, 2004). However, the phylogenetic analysis obtained with these markers individually is limited because no gene amplification is obtained for a few

species, and some closely related species are difficult to differentiate, like those belonging to MTBC complex (Mignard & Flandrois, 2007).

Recently, multigene sequence analysis was applied to mycobacteria, revealing novel insights into the phylogenetic relationships between the various *Mycobacterium* species. Devulder *et al.* (2005) developed a multigene sequence database incorporating four genes (16S rRNA gene, *hsp65*, *rpoB*, and *sodA*) within the *Mycobacterium* genus. The concatenation of four genes provides a good tool of increasing the robustness of the final tree, but presented some inaccuracies, especially for MTBC complex (Devulder *et al.*, 2005). Another tree based on the combination of 16S rRNA gene, *rpoB*, *recA*, *hsp65*, and *sodA* was performed by Adékambi & Drancourt (2004) with good bootstrap support; however, the same authors showed that the trees based only on one of these genes were not very robust. Recently, the *tuf* gene coding for EF-TU factor was proposed as phylogenetic marker, and the corresponding tree was quite robust (Mignard & Flandrois, 2007).

Therefore, phylogenetic analyses based on the combined dataset of a panel of gene sequences could help to delineate new mycobacterial species, as well as enabling the monitoring of drug resistance-conferring mutations (Adékambi & Drancourt, 2004). In this context, the *M. tuberculosis dprE1* might represent an interesting candidate as it is an essential gene (Sassetti & Rubin, 2003), and it encodes a 'hot' target of five new antitubercular agents, including the benzothiazinones (BTZs; Makarov *et al.*, 2009; Christophe *et al.*, 2009; Magnet *et al.*, 2010; Stanley *et al.*, 2012; Wang *et al.*, 2013). DprE1 enzyme works in concert with DprE2, and it is involved in the biosynthesis of arabinogalactan, an essential component of the mycobacterial cell wall core (Wolucka, 2008). It has been demonstrated that point mutations responsible for the substitution of Cys387 residue of *M. tuberculosis* DprE1 are responsible for BTZ resistance (Makarov *et al.*, 2009). This cysteine residue is highly conserved in orthologous DprE1 proteins from various BTZ-susceptible Actinobacteria; on the other site, in *Mycobacterium avium* and *Mycobacterium aurum*, the Cys387 residue is replaced by serine or alanine, respectively (Makarov *et al.*, 2009); this achievement renders bacteria belonging to these species naturally resistant to BTZ. Accordingly, DprE1 might represent a valuable phylogenetic and/or taxonomic marker, and its possible role in this context was investigated in this work.

Materials and methods

Bacterial strains and growth conditions

The type strains of nine mycobacterial species, *Mycobacterium africanum* (ATCC 25420), *Mycobacterium xenopi* (ATCC 192509), *Mycobacterium intracellulare* (ATCC 13209), *Mycobacterium avium* subsp. *paratuberculosis* (ATCC 19698), *Mycobacterium scrofulaceum* (ATCC 19073), *Mycobacterium chelonae* (ATCC 14472), *Mycobacterium celatum* (ATCC 51130), *Mycobacterium gastri* (ATCC 15754), and *Mycobacterium simiae* (ATCC 25273) were purchased from the American Type Culture Collection (ATCC). These strains were grown either in Middlebrook 7H9 broth (Difco) with 0.05% Tween 80 or on Middlebrook 7H11 agar (Difco) with 0.5% glycerol, both supplemented with 10% (vol/vol) OADC or on Lowenstein–Jensen medium, following the instructions of ATCC Web site (http://www.lgcstandards-atcc.org/). Mycobacterial cultures were usually grown at 37 °C without shaking for 3–4 weeks, with the exception of *M. chelonae*, which was grown in the same conditions for about 4 days.

PCR primers and cloning

Gene-specific and species-specific PCR primers were designed (Table 1) and *dprE1* orthologous genes were amplified by PCR, using the cell lysates of each mycobacterial strain as template. PCR experiments were carried out using STAT-NAT DNA-Mix kit (STabilized Amplification Technology Nucleic Acid Testing, Sentinel CH SpA, Italy; composition: 3.0 mM $MgCl_2$, 0.8 mM dNTPs, 2u Hot Start Taq Polymerase). Amplicons were purified using the Wizard SV Gel and PCR clean-up system (Promega) and then cloned in pGEM-T Easy vector (Promega). The nucleotide sequence of the insert of recombinant plasmids (*dprE1*/pGEM-T) was determined by Sanger sequencing (www.bmr-genomics.it/).

The nine *dprE1* gene sequences not available in databases were deposited at NCBI Web site (http://www.ncbi.nlm.nih.gov/) and were assigned the accession numbers reported in Table 1.

Sequence analysis

Amino acid sequences of putative DprE1 proteins were retrieved using the *M. tuberculosis* DprE1 amino acid sequence (GI:15610926) as a query to probe the nonredundant protein sequences (nr) database at NCBI site using BLASTP (Altschul *et al.*, 1997). Only those sequences retrieved at an *E*-value below the 0.05 threshold were taken into account. Amino acid sequences of Hsp65 and RpoB proteins were retrieved from the NCBI database and trimmed as found in bibliography (Telenti *et al.*, 1993; Adékambi *et al.*, 2003). The MUSCLE program was used to perform the amino acid multialignment (Edgar, 2004). Alignments were manually checked, and misaligned regions were removed.

Table 1. Oligonucleotides for cloning and sequencing mycobacterial *dprE1* genes

Oligonucleotides	Sequence (5′–3′)	Species	Accession number
Mafri forward	CGCCACGGTAATCAACTTCATC	*M. africanum*	KC588931
Mafri reverse	GCAGGTAGCGCTCGCAGATG		
M.int forward	GATTACCCGCCTCCTCAGC	*M. intracellulare*	KC588933
M.int reverse	AGGTAGCGCTCGCAAATGG		
M.avi forward	TACCCTCTTTCACGATGTCG	*M. scrofulaceum*	JX215333
M.avi reverse	CGGCGTCCAGCACCATCTAG		
M.abs forward	TGAGGACAAGCCATGGCGCGT	*M. chelonae*	JX215336
M.absc reverse	CCGATCTCCGAGGTGCCGC		
M.avi forward	TACCCTCTTTCACGATGTCG	*M. a.* subsp. *paratuberculosis*	KC588934
M.avi reverse	CGGCGTCCAGCACCATCTAG		
2KFor2 forward	CTVGGCMGSTCCTAYGGSGA	*M. xenopi*	KC588932
2KRev reverse	TCSARSCGKCGGGCCATGTC		
2KFor2 forward	CTVGGCMGSTCCTAYGGSGA	*M. celatum*	JX215332
2KRev reverse	TCSARSCGKCGGGCCATGTC		
2KFor2 forward	CTVGGCMGSTCCTAYGGSGA	*M. gastri*	X215335
2KRev reverse	TCSARSCGKCGGGCCATGTC		
2KFor2 forward	CTVGGCMGSTCCTAYGGSGA	*M. simiae*	JX215334
2KRev reverse	TCSARSCGKCGGGCCATGTC		
Ntb1 forward	GCAGCGAGCCGTGATCTTCCG	*M. a.* subsp. *paratuberculosis*,	–
Ntb2 Reverse	CGAATTGTGCAGGTAGCGCTC	*M. xenopi*, *M. celatum*, *M. gastri*, *M. simiae*	

The ConSurf server was used for the evaluation of the evolutionary conservation of amino acid positions in the DprE1 proteins, based on the phylogenetic relations between orthologous sequences (Glaser *et al.*, 2003). The multialignment of the 73 DprE1 amino acid sequences was used to perform a phylogenetic tree by the neighbor-joining algorithm as implemented in the Rate4Site program (Pupko *et al.*, 2002). Position-specific conservation scores were, then, computed by the empirical Bayesian approach (Mayrose *et al.*, 2004). Finally, the conservation scores were projected onto the *Mycobacterium smegmatis* DprE1 protein structure (PDB: 4f4q; Neres *et al.*, 2012).

Phylogenetic analysis

Neighbor-joining (NJ) phylogenetic trees (Saitou & Nei, 1987) were obtained with Mega5, using pairwise deletion option and 1000 bootstrap replicates (Tamura *et al.*, 2011).

A concatamer was obtained adopting the following procedure: (1) the orthologs of FusA (protein chain elongation factor EF-G), IleS (isoleucyl-tRNA synthetase), LepA (back-translocating elongation factor EF4), LeuS (leucyl-tRNA synthetase), PyrG (CTP synthetase), RecA (recombinase A), RecG (ATP-dependent DNA helicase), RplB (50S ribosomal protein L2) and RpoB (RNA polymerase beta subunit; Santos & Ochman, 2004) of *M. tuberculosis* H37Rv strain [sequences recovered from the RDP Resource Download Area at Ribosomal Database project site (http://rdp.cme.msu.edu/)] were retrieved from 46 mycobacterial genomes; (2) each ortholog dataset was independently aligned; and (3) all the different multialignments were concatenated in a single one comprising 7833 residues. The concatenated sequences of the same genes of *Corynebacterium efficiens* YS314 were used as an out-group.

Results and discussion

PCR amplification and sequencing of *dprE1* orthologous genes from strains belonging to nine *Mycobacterium* species

Nine *dprE1* genes of *M. africanum*, *M. xenopi*, *M. intracellulare*, *M. avium* subsp. *paratuberculosis*, *M. scrofulaceum*, *M. chelonae*, *M. celatum*, *M. gastri*, and *M. simiae* species were amplified by PCR using *ad hoc*-designed gene-specific primers reported in Table 1. The *dprE1* amplicons obtained were then cloned in pGEM-T Easy plasmid vector, and their nucleotide sequences were determined as described in Materials and methods. The nine *dprE1* gene sequences obtained were submitted to NCBI Web site, and the corresponding accession numbers were reported in Table 1. These sequences were utilized for further analyses.

Identification of both DprE1 mycobacterial proteins and putative mycobacterial BTZ-susceptible and BTZ-resistant species

To check the phylogenetic distribution of the DprE1-like proteins in the entire *Mycobacterium* genus, the *M. tuberculosis* DprE1 amino acid sequence (GI:15610926) was used as a query to probe the nr NCBI database. In this way, a total of 64 sequences homologous to *M. tuberculosis* DprE1 were retrieved and aligned with the nine ones obtained in this work (DprE1 of *M. africanum*, *M. xenopi*, *M. intracellulare*, *M. avium* subsp. *paratuberculosis*, *M. scrofulaceum*, *M. chelonae*, *M. celatum*, *M. gastri*, and *M. simiae*). The corresponding multialignment of 73 DprE1 amino acid sequences is reported as Supporting Information, Data S1. The analysis revealed a high degree of sequence conservation between DprE1 proteins belonging to different mycobacterial species. This similarity is highlighted in Fig. 1, obtained using the ConSurf server (Glaser *et al.*, 2003). In this picture, the conservation scores of each amino acid at each positions are projected onto the *M. smegmatis* DprE1 protein structure (PDB: 4f4q; Neres *et al.*, 2012). In Fig. 1b, all residues having the highest degree of conservation are highlighted.

To identify the conservation degree of amino acids located into the DprE1 active site, twelve residues from *M. smegmatis* DprE1 structure (Tyr67, His139, Gly140, Lys141, Lys425, Gln341, Gln343, Leu370, Lys374, Phe376, Asn392, and Cys394) were analyzed in the 73 mycobacterial species (Neres *et al.*, 2012). Eleven of these twelve residues are conserved in all analyzed sequences; the only exception is represented by Cys394 (Cys387 in *M. tuberculosis*) that, in some sequences, is replaced by an alanine. Because the presence of cysteine (Cys394 in *M. smegmatis* and Cys387 in *M. tuberculosis*) is clearly associated to BTZ sensitivity (Makarov *et al.*, 2009; Neres *et al.*, 2012), the 11 mycobacterial species (*M. abscessus*, *M. massiliense*, *M. chelonae*, *M. rhodesiae*, *M. tusciae*, *M. neoaurum*, *M. parascrofulaceum*, *M. avium subsp. avium*, *M. avium subsp. paratuberculosis*, *M. colombiense*, and *M. intracellulare*), having an Ala replacing a Cys in this position, are very likely resistant to BTZs. This result is in agreement with previous experimental findings, showing that strains belonging to the two species *M. avium* and *M. aurum* are naturally resistant to BTZs (Makarov *et al.*, 2009).

It is noteworthy that among the 11 conserved amino acids, His139, Lys425, and Gln343 residues are essential for FAD binding and critical for full enzyme activity, as it was demonstrated by structural and enzymatic assays (Neres *et al.*, 2012).

DprE1 phylogenetic analysis

The multialignment of DprE1 amino acid sequences (Data S1) was used to build the neighbor-joining tree shown in Fig. 2. The analysis of the DprE1 tree revealed that different strains of the same species shared a high degree of sequence similarity and were clustered together in the tree, except for the *Mycobacterium rhodesiae* and *M. xenopi* strains (Fig. 2). At the same time, each species is clearly separated from each other. The topology of the DprE1 tree is different from those obtained with other molecular markers for the branching order of some mycobacterial species (Tortoli, 2012). However, most nodes in the DprE1 tree were supported by high bootstrap values (Fig. 2).

All these data strongly suggest the possibility to use *DprE1* as a taxonomic marker for identifying/clustering strains belonging to the same mycobacterial species. Nonetheless, in our opinion, the most important feature of the DprE1 phylogenetic analysis is related to the BTZ sensitivity/resistance of mycobacterial strains. In fact, in

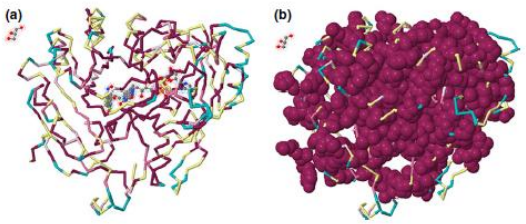

Fig. 1. Conservation scores of amino acid at each position projected onto the *Mycobacterium smegmatis* DprE1 protein structure. (a) Conservation scores, obtained with ConSurf server (Glaser *et al.*, 2003), of each amino acid at each positions are projected onto the *M. smegmatis* DprE1 protein structure (PDB: 4f4q; Neres *et al.*, 2012). The continuous conservation scores are divided into a discrete scale of nine grades for visualization, from the most variable positions (grade 1) colored turquoise, through intermediately conserved positions (grade 5) colored white, to the most conserved positions (grade 9) colored maroon. In (b) Only residues having the highest degree of conservation are highlighted.

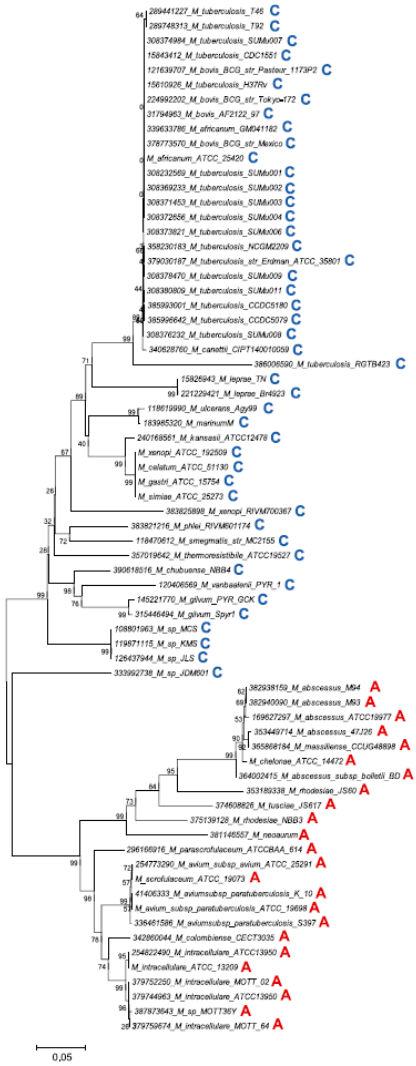

Fig. 2. Phylogenetic tree constructed with the amino acid sequences of 73 homologous to *Mycobacterium tuberculosis* DprE1. Neighbor-joining (NJ) phylogenetic tree was obtained with Mega5 (Tamura *et al.*, 2011), pairwise deletion option, and 1000 bootstraps replicates. C, cysteine; A, alanine.

the DprE1 tree, it is possible to discriminate two different clusters, each of which including mycobacterial species having Cys or Ala in position 387. It is underlined that beside BTZs, other three molecules, DNB1, VI-9376, and 377790, have been published to form covalent bonds with the cysteine residue within the active site of DprE1, thus blocking the enzymatic activity (Christophe *et al.*, 2009; Makarov *et al.*, 2009; Magnet *et al.*, 2010; Stanley *et al.*, 2012). Until now, only one DprE1 inhibitor is able to form a noncovalent binding with Cys387 (Wang *et al.*, 2013). The first cluster (having Cys387) comprised the following species: MTBC, *M. leprae*, *M. ulcerans*, *M. marinum*, *M. kansasii*, *M. xenopi*, *M. celatum*, *M. gastri*, *M. simiae*, *M. phlei*, *M. smegmatis*, *M. thermoresistibile*, *M. chubuense*, *M. vanbalenii*, and *M. gilvum*. On the basis of the available data, strains belonging to these species might be susceptible to BTZs as well as to the other three DprE1 inhibitors. In fact, it is noteworthy that *M. tuberculosis* H37Rv (moreover 240 clinical isolates comprising MDR and XDR strains), *M. bovis*, *M. smegmatis*, and *M. marinum* are susceptible to BTZs (Makarov *et al.*, 2009; Pasca *et al.*, 2010). The second cluster (exhibiting an Ala387) embedded the following species whose

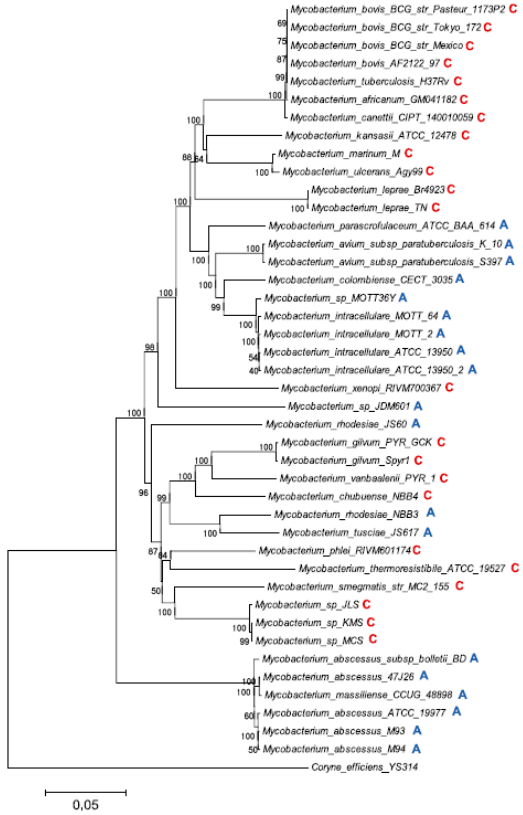

Fig. 3. Phylogenetic tree constructed using the concatenated sequences of nine proteins belonging to 46 different *Mycobacterium* strains. The concatamer was obtained using the orthologs of FusA, IleS, LepA, LeuS, PyrG, RecA, RecG, RplB, and RpoB of *M. tuberculosis* H37Rv strain.

representatives might be resistant to BTZs: *M. abscessus*, *M. massiliense*, *M. chelonae*, *M. abscessus subsp. bolletii*, *M. rhodesiae*, *M. tusciae*, *M. neoaurum*, *M. parascrofulaceum*, and MAC (Fig. 2). Among these cited species, *M. avium* was tested to be resistant to BTZs (Makarov *et al.*, 2009). The presence of either a Cys or an Ala residue might, in principle, be a powerful tool to indicate whether a mycobacterial species is susceptible/resistant to BTZs and to the other DprE1 inhibitors DNB1, VI-9376, and 377790.

Consequently, the amino acid localized at position 387 should be critical for the resistance/sensitivity to BTZs. To check the influence of such residues (Cys or Ala) at position 387 on the topology of the DprE1 tree, an additional phylogenetic tree was constructed using the original DprE1 amino acid sequences and the 'chimeric' ones where the Cys387 was replaced by an Ala and *vice versa* (Data S2). The analysis of the DprE1 phylogenetic tree embedding also the 'chimeric' sequences revealed that, as might be expected, its topology was identical to that of the tree constructed with the original sequences (Data S2; Fig. 2).

Phylogenetic analysis

The analysis of DprE1 tree raised the question of the possible congruence existing between these data and the overall *Mycobacterium* phylogeny, an issue yet under debate. Indeed, the *Mycobacterium* genus is characterized by a very limited interspecies genetic variability, and this is the cause of a problematic phylogenetic reconstruction (Tortoli, 2012).

Consequently, a phylogenetic tree was constructed from the alignment of the concatenated amino acid sequences of the products of nine housekeeping genes (Santos & Ochman, 2004), as recommended on the site of Ribosomal Database Project as universally conserved genes that can be used for identification and phylogenetic analysis of bacteria (see Materials and methods; Data S3) from 46 *Mycobacterium* strains (Santos & Ochman, 2004; Fig. 3).

The analysis of the concatamer tree revealed that strains belonging to the same species were clustered together, whereas different species are clearly separated. It is quite interesting that nodes separating different species are supported by very high bootstrap values (99–100%; Fig. 3). Both the robust topology and high bootstraps suggest that the concatamer tree is much more reliable for other trees constructed using single genes, such as those based on complete 16S rRNA gene sequences or on the amino acid sequences coded by fragments of *hsp65* and *rpoB* genes (Telenti *et al.*, 1993; Adékambi *et al.*, 2003; Data S4).

The only exception is represented by *M. rhodesiae* J60 and NBB3 strains that are not clustered together (Fig. 3), like in the DprE1 tree, previously described (Fig. 2). Also in this tree, the related species were clustered in MTBC or MAC complexes (Fig. 3).

Moreover, there is no a separation between the mycobacterial BTZ-susceptible and BTZ-resistant species. Consequently, this parameter is not linked to the phylogeny of mycobacteria.

Conclusions

The aim of this work was to check the possibility of using the *dprE1* gene as a new molecular marker for taxonomical and/or phylogenetic studies of mycobacteria. The whole body of data obtained suggested that *DprE1* tree might represent an additional good taxonomic marker for the assignment of a mycobacterial isolate to a given species. In addition, the same marker might also give insights into sensitivity/resistance of mycobacterial isolates to BTZs and to other drugs hitting DprE1 enzyme, simply checking for the presence/absence in position 387 of Cys residue, respectively.

Lastly, the phylogenetic tree, constructed using a concatamer of nine housekeeping genes, was supported by very high bootstrap values. Consequently, this tree represents a good reference phylogeny for the *Mycobacterium* genus.

Acknowledgement

This work was supported by European Commission (VII Framework, contract no. 260872).

Authors' contribution

M.L.I. and E.P. contributed equally to this work.

References

Adékambi T & Drancourt M (2004) Dissection of phylogenetic relationships among 19 rapidly growing *Mycobacterium* species by 16S rRNA, *hsp65*, *sodA*, *recA* and *rpoB* gene sequencing. *Int J Syst Evol Microbiol* **54**: 2095–2105.

Adékambi T, Colson P & Drancourt M (2003) *rpoB*-based identification of nonpigmented and late-pigmenting rapidly growing mycobacteria. *J Clin Microbiol* **41**: 5699–5708.

Altschul SF, Madden TL, Schaffer AA, Zhang J, Zhang Z, Miller W & Lipman DJ (1997) Gapped BLAST and PSI-BLAST: a new generation of protein database search programs. *Nucleic Acids Res* **25**: 3389–3402.

Bouakaze C, Keyser C, Gonzalez A, Sougakoff W, Veziris N, Dabernat H, Jaulhac B & Ludes B (2011) Matrix-assisted laser desorption ionization-time of flight mass spectrometry-based single nucleotide polymorphism genotyping assay using iPLEX gold technology for identification of *Mycobacterium tuberculosis* complex species and lineages. *J Clin Microbiol* **49**: 3292–3299.

Christophe T, Jackson M, Jeon HK *et al.* (2009) High content screening identifies decaprenyl-phosphoribose 2' epimerase as a target for intracellular antimycobacterial inhibitors. *PLoS Pathog* **5**: e1000645.

Devulder G, Pérouse de Montclos M & Flandrois JP (2005) A multigene approach to phylogenetic analysis using the genus *Mycobacterium* as a model. *Int J Syst Evol Microbiol* **55**: 293–302.

Edgar RC (2004) MUSCLE: multiple sequence alignment with high accuracy and high throughput. *Nucleic Acids Res* **32**: 1792–1797.

Field SK & Cowie RL (2006) Lung disease due to the more common nontuberculous mycobacteria. *Chest* **129**: 1653–1672.

Glaser F, Pupko T, Paz I, Bell RE, Bechor-Shental D, Martz E & Ben-Tal N (2003) ConSurf: identification of functional regions in proteins by surface-mapping of phylogenetic information. *Bioinformatics* **19**: 163–164.

Magnet S, Hartkoorn RC, Székely R *et al.* (2010) Leads for antitubercular compounds from kinase inhibitor library screens. *Tuberculosis* **90**: 354–360.

Makarov V, Manina G, Mikusova K *et al.* (2009) Benzothiazinones kill *Mycobacterium tuberculosis* by blocking arabinan synthesis. *Science* **324**: 801–804.

Mayrose I, Graur D, Ben-Tal N & Pupko T (2004) Comparison of site-specific rate-inference methods for protein sequences: empirical Bayesian methods are superior. *Mol Biol Evol* **21**: 1781–1791.

Mignard S & Flandrois JP (2007) Identification of *Mycobacterium* using the EF-Tu encoding (*tuf*) gene and the tmRNA encoding (*ssrA*) gene. *J Med Microbiol* **56**: 1033–1041.

Neres J, Pojer F, Molteni E *et al.* (2012) Structural basis for benzothiazinone-mediated killing of *Mycobacterium tuberculosis*. *Sci Transl Med* **4**: 150ra121.

Pasca MR, Degiacomi G, Ribeiro AL *et al.* (2010) Clinical isolates of *Mycobacterium tuberculosis* in four European hospitals are uniformly susceptible to benzothiazinones. *Antimicrob Agents Chemother* **54**: 1616–1618.

Pupko T, Bell RE, Mayrose I, Glaser F & Ben-Tal N (2002) Rate4Site: an algorithmic tool for the identification of functional regions in proteins by surface mapping of evolutionary determinants within their homologues. *Bioinformatics* **18**: S71–S77.

Saitou N & Nei M (1987) The neighbor-joining method: a new method for reconstructing phylogenetic trees. *Mol Biol Evol* **4**: 406–425.

Santos SR & Ochman H (2004) Identification and phylogenetic sorting of bacterial lineages with universally conserved genes and proteins. *Environ Microbiol* **6**: 754–759.

Sassetti CM & Rubin EJ (2003) Genetic requirements for mycobacterial survival during infection. *P Natl Acad Sci USA* **100**: 12989–12994.

Stanley SA, Grant SS, Kawate T *et al.* (2012) Identification of novel inhibitors of *M. tuberculosis* growth using whole cell based high-throughput screening. *ACS Chem Biol* **7**: 1377–1384.

Suzuki K, Akama T, Kawashima A, Yoshihara A, Yotsu RR & Ishii N (2012) Current status of leprosy: epidemiology, basic science and clinical perspectives. *J Dermatol* **39**: 121–129.

Tamura K, Peterson D, Peterson N, Stecher G, Nei M & Kumar S (2011) MEGA5: molecular evolutionary genetics analysis using maximum likelihood, evolutionary distance, and maximum parsimony methods. *Mol Biol Evol* **28**: 2731–2739.

Telenti A, Marchesi F, Balz M, Bally F, Böttger EC & Bodmer T (1993) Rapid identification of mycobacteria to the species level by polymerase chain reaction and restriction enzyme analysis. *J Clin Microbiol* **31**: 175–178.

Tortoli E (2012) Phylogeny of the genus *Mycobacterium*: many doubts, few certainties. *Infect Genet Evol* **12**: 827–831.

Wang F, Sambandan D, Halder R *et al.* (2013) Identification of a small molecule with activity against drug-resistant and persistent tuberculosis. *P Natl Acad Sci USA* **110**: E2510–E2517.

Wolucka BA (2008) Biosynthesis of D-arabinose in mycobacteria - a novel bacterial pathway with implications for antimycobacterial therapy. *FEBS J* **275**: 2691–2711.

Supporting Information

Additional Supporting Information may be found in the online version of this article:

Data S1. DprE1 sequences multialignment (Multialignment of 73 DprE1 amino acid sequences used in this work).

Data S2. Phylogenetic tree of DprE1 chimeric sequences (Phylogenetic tree constructed with both the original DprE1 sequences and the chimeric DprE1 sequences).

Data S3. Concatenated sequences multialignment (Multialignment of the concatenated amino acid sequences of nine housekeeping genes of 46 *Mycobacterium* strains).

Data S4. Phylogenetic tree of the 16S rRNA gene, Hsp65 and RpoB sequences of 46 *Mycobacterium* strains (Description of data: Neighbor-Joining (NJ) phylogenetic trees were obtained with Mega5 (Tamura *et al.*, 2011), pairwise deletion option and 1000 bootstraps replicates. Phylogenetic trees were constructed using: (a) the complete 16S rRNA gene sequences; (b) the amino acid sequences coded by fragments of Hsp65 (Telenti *et al.*, 1993); (c) RpoB (Adékambi *et al.*, 2003) proteins of 46 *Mycobacterium* strains whose genome was present in the database).

Bibliography

Adekambi, T. & M. Drancourt, (2004) Dissection of phylogenetic relationships among 19 rapidly growing *Mycobacterium* species by 16S rRNA, hsp65, sodA, recA and rpoB gene sequencing. *Int J Syst Evol Microbiol* **54**: 2095-2105.

Bond, D. R. & D. R. Lovley, (2003) Electricity production by *Geobacter sulfurreducens* attached to electrodes. *Appl Environ Microbiol* **69**: 1548-1555.

Bond, D. R., S. M. Strycharz-Glaven, L. M. Tender & C. I. Torres, (2012) On electron transport through *Geobacter* biofilms. *ChemSusChem* **5**: 1099-1105.

Bouakaze, C., C. Keyser, A. Gonzalez, W. Sougakoff, N. Veziris, H. Dabernat, B. Jaulhac & B. Ludes, (2011) Matrix-assisted laser desorption ionization-time of flight mass spectrometry-based single nucleotide polymorphism genotyping assay using iPLEX gold technology for identification of *Mycobacterium tuberculosis* complex species and lineages. *J Clin Microbiol* **49**: 3292-3299.

Christophe, T., M. Jackson, H. K. Jeon, D. Fenistein, M. Contreras-Dominguez, J. Kim, A. Genovesio, J. P. Carralot, F. Ewann, E. H. Kim, S. Y. Lee, S. Kang, M. J. Seo, E. J. Park, H. Skovierova, H. Pham, G. Riccardi, J. Y. Nam, L. Marsollier, M. Kempf, M. L. Joly-Guillou, T. Oh, W. K. Shin, Z. No, U. Nehrbass, R. Brosch, S. T. Cole & P. Brodin, (2009) High content screening identifies decaprenyl-phosphoribose 2' epimerase as a target for intracellular antimycobacterial inhibitors. *PLoS Pathog* **5**: e1000645.

Devulder, G., M. Perouse de Montclos & J. P. Flandrois, (2005) A multigene approach to phylogenetic analysis using the genus *Mycobacterium* as a model. *Int J Syst Evol Microbiol* **55**: 293-302.

Du, Z., H. Li & T. Gu, (2007) A state of the art review on microbial fuel cells: A promising technology for wastewater treatment and bioenergy. *Biotechnol Adv* **25**: 464-482.

Field, S. K. & R. L. Cowie, (2006) Lung disease due to the more common nontuberculous mycobacteria. *Chest* **129**: 1653-1672.

Kim, B. H., I. S. Chang & G. M. Gadd, (2007) Challenges in microbial fuel cell development and operation. *Appl Microbiol Biotechnol* **76**: 485-494.

Logan, B. E., (2010) Scaling up microbial fuel cells and other bioelectrochemical systems. *Appl Microbiol Biotechnol* **85**: 1665-1671.

Logan, B. E., C. Murano, K. Scott, N. D. Gray & I. M. Head, (2005) Electricity generation from cysteine in a microbial fuel cell. *Water Res* **39**: 942-952.

Logan, B. E. & J. M. Regan, (2006) Electricity-producing bacterial communities in microbial fuel cells. *Trends Microbiol* **14**: 512-518.

Lovley, D. R., (2006) Bug juice: harvesting electricity with microorganisms. *Nat Rev Microbiol* **4**: 497-508.

Magnet, S., R. C. Hartkoorn, R. Szekely, J. Pato, J. A. Triccas, P. Schneider, C. Szantai-Kis, L. Orfi, M. Chambon, D. Banfi, M. Bueno, G. Turcatti, G. Keri & S. T. Cole, (2010) Leads for antitubercular compounds from kinase inhibitor library screens. *Tuberculosis (Edinb)* **90**: 354-360.

Makarov, V., G. Manina, K. Mikusova, U. Mollmann, O. Ryabova, B. Saint-Joanis, N. Dhar, M. R. Pasca, S. Buroni, A. P. Lucarelli, A. Milano, E. De Rossi, M. Belanova, A. Bobovska, P. Dianiskova, J. Kordulakova, C. Sala, E. Fullam, P. Schneider, J. D. McKinney, P. Brodin, T. Christophe, S. Waddell, P. Butcher, J. Albrethsen, I. Rosenkrands, R. Brosch, V. Nandi, S. Bharath, S. Gaonkar, R. K. Shandil, V. Balasubramanian, T. Balganesh, S. Tyagi, J. Grosset, G. Riccardi & S. T. Cole, (2009) Benzothiazinones kill *Mycobacterium tuberculosis* by blocking arabinan synthesis. *Science* **324**: 801-804.

Mignard, S. & J. P. Flandrois, (2007) Identification of *Mycobacterium* using the EF-Tu encoding (tuf) gene and the tmRNA encoding (ssrA) gene. *J Med Microbiol* **56**: 1033-1041.

Rabaey, K. & W. Verstraete, (2005) Microbial fuel cells: novel biotechnology for energy generation. *Trends Biotechnol* **23**: 291-298.

Stanley, S. A., S. S. Grant, T. Kawate, N. Iwase, M. Shimizu, C. Wivagg, M. Silvis, E. Kazyanskaya, J. Aquadro, A. Golas, M. Fitzgerald, H. Dai, L. Zhang & D. T. Hung, (2012) Identification of novel inhibitors of *M. tuberculosis* growth using whole cell based high-throughput screening. *ACS Chem Biol* **7**: 1377-1384.

Suzuki, K., T. Akama, A. Kawashima, A. Yoshihara, R. R. Yotsu & N. Ishii, (2012) Current status of leprosy: epidemiology, basic science and clinical perspectives. *J Dermatol* **39**: 121-129.

Wang, H., R. B. Sessions, S. S. Prime, D. K. Shoemark, S. J. Allen, W. Hong, S. Narayanan & I. C. Paterson, (2013) Identification of novel small molecule TGF-beta antagonists using structure-based drug design. *J Comput Aided Mol Des* **27**: 365-372.

Wolucka, B. A., (2008) Biosynthesis of D-arabinose in mycobacteria - a novel bacterial pathway with implications for antimycobacterial therapy. *FEBS J* **275**: 2691-2711.